TOMSK STATE UNIVERSITY

Chromium-Compensated GaAs X-ray Sensors

March 25-27, 2015
Stanford, CA, US


Зоны Internet
СЕВЕРНАЯ АМЕРИКА
ЕВРОПА
РОССИЯ
АЗИЯ
АФРИКА
ЮЖНАЯ АМЕРИКА
АВСТРАЛИЯ
Санкт - Петербург
Москва

Tomsk





HOTEL

Functional Electronics Laboratory (FEL) of Tomsk State University

R&D activities of FEL:

- GaAs:Cr radiation imaging sensors;
- Nonlinear optic crystal growth (GaSe, $ZnGeP_2$);
- LED based on GaN/GaInN structures.

You Are Welcome to FEL !

X-ray absorption coefficients for Si, GaAs, and CdTe/ $Cd_{1-x}Zn_xTe$ material

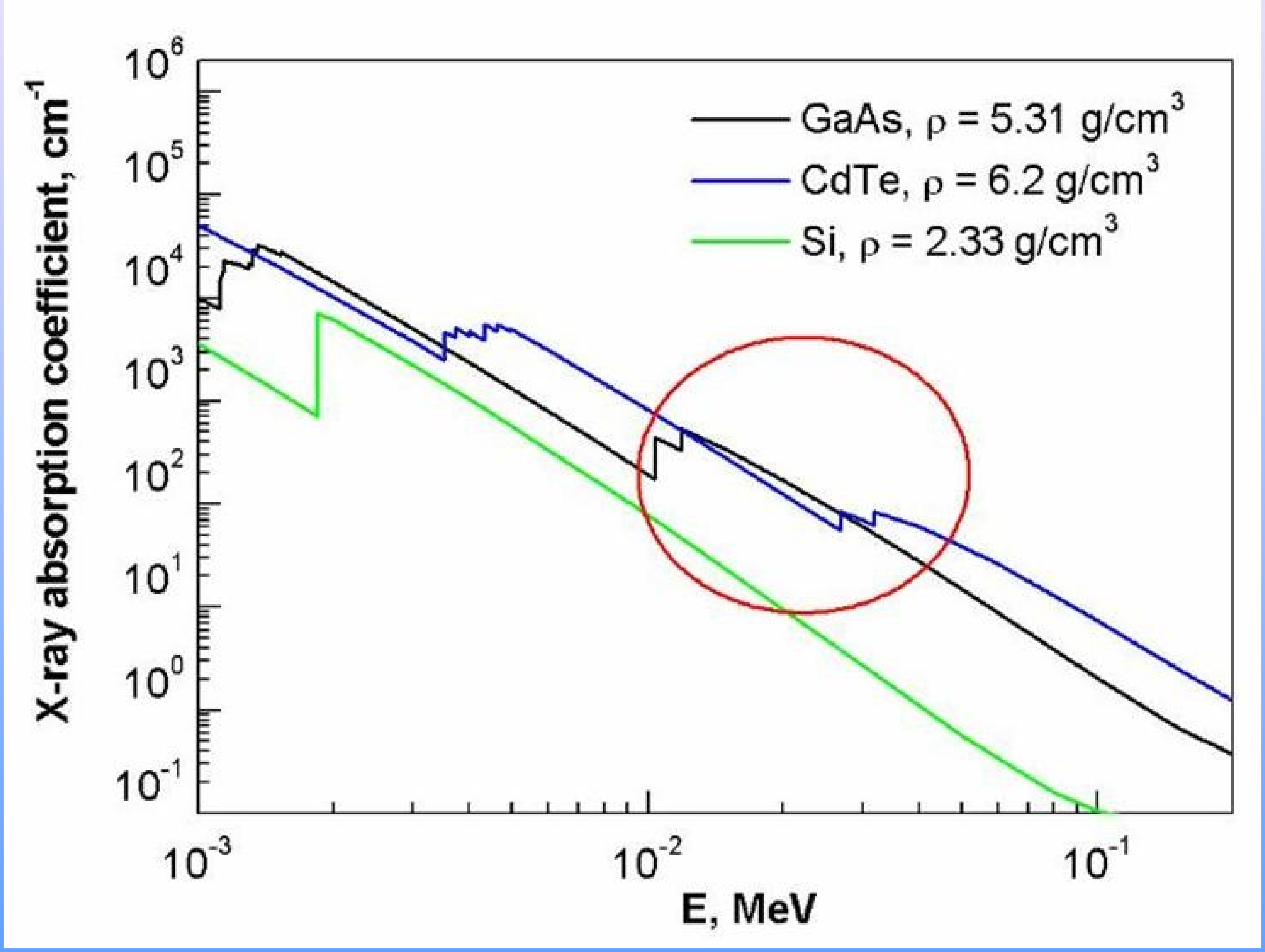

Technology of HR GaAs

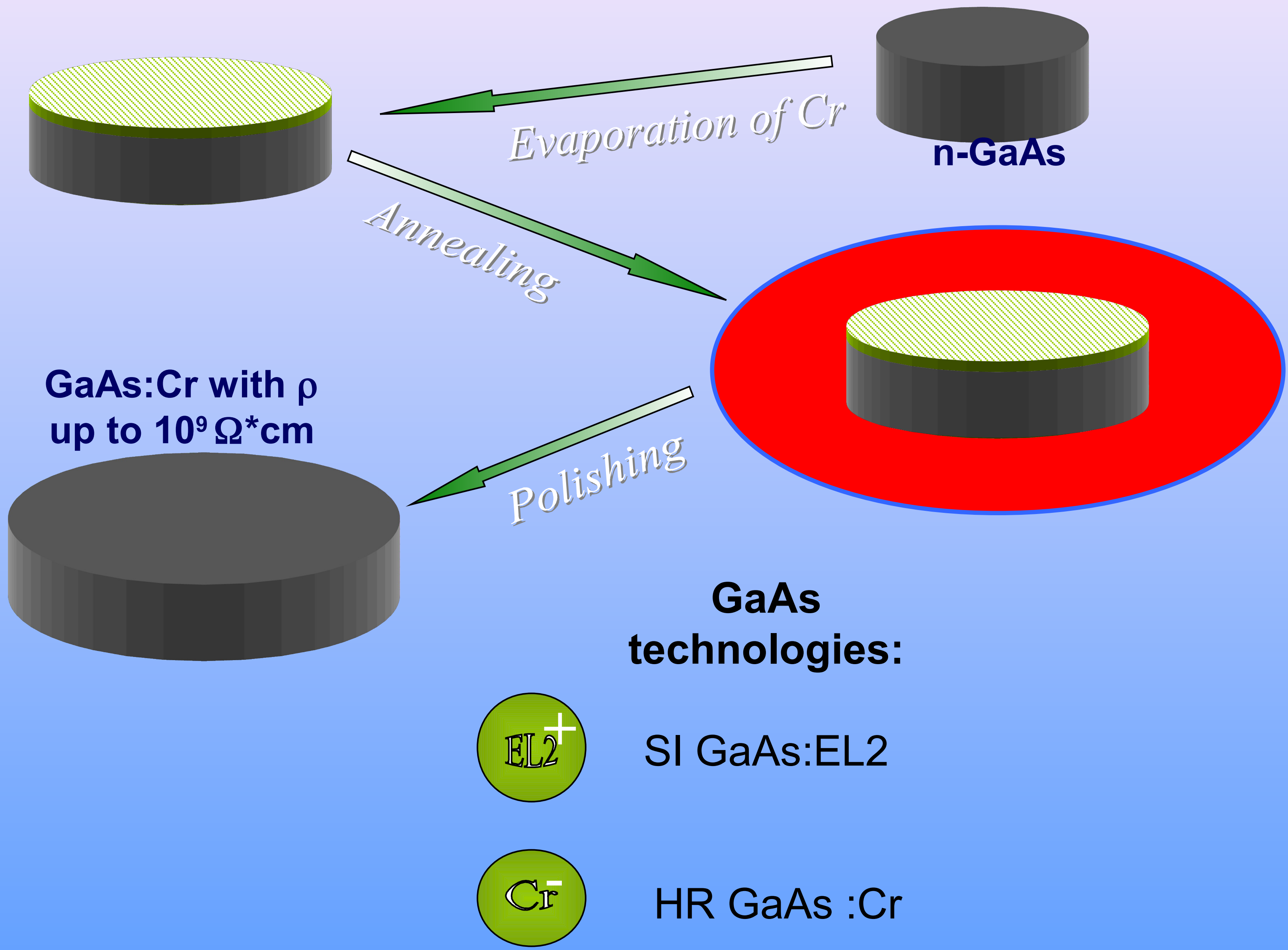

Electrophysical characteristics

Material	Conductivity $10^{-9} \times (\Omega cm)^{-1}$	n_o 10^5 cm^{-3}	p_o 10^5 cm^{-3}	Electron mobility μ_n, cm^2/ Vs	Hole mobility μ_p, cm^2/ Vs
SI GaAs (GaAs:EL2)	6 - 9	70 - 100	4 - 6	5100-5800	340 - 390
HR GaAs (GaAs:Cr)	0.6 - 1.1	2 - 3	120-200	3200-4700	210 - 320

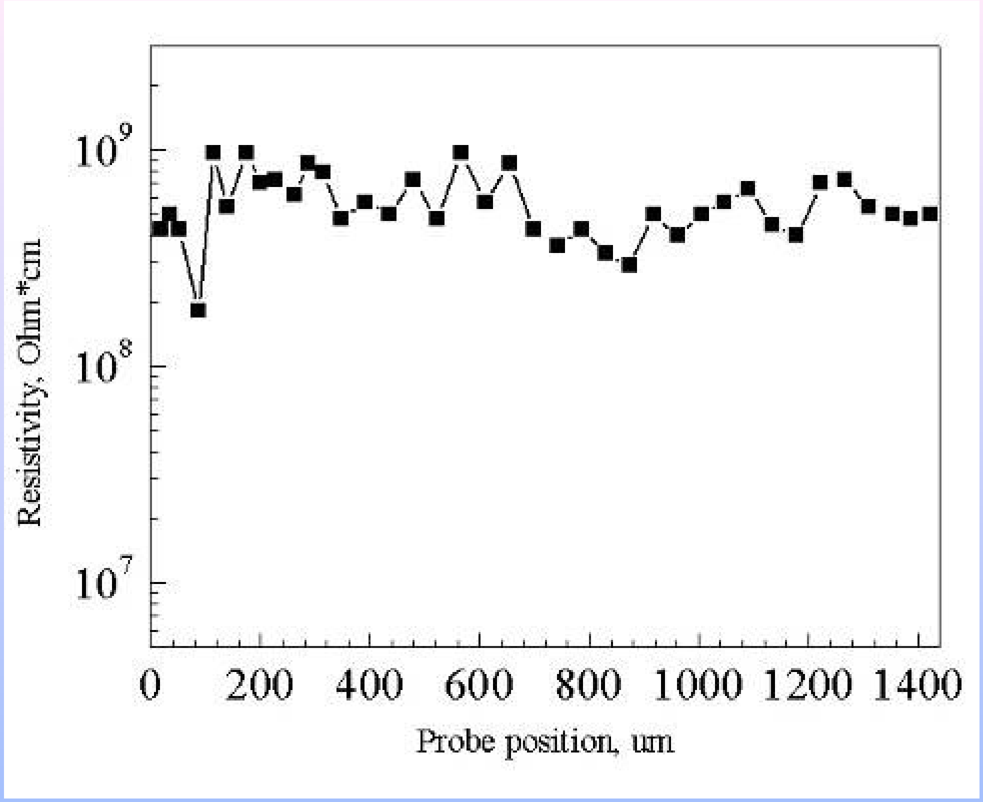

Resistivity distribution through the HR GaAs wafer thickness.
Estimation made from current-voltage characteristics of a point contact

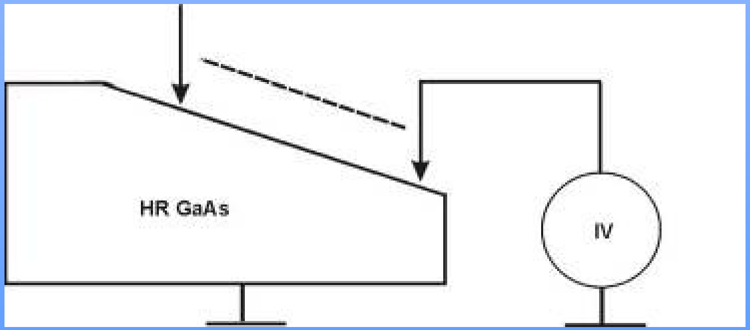

Resistivity mapping on 40 mm HR GaAs wafer. Corema RM system (non contact measurement).

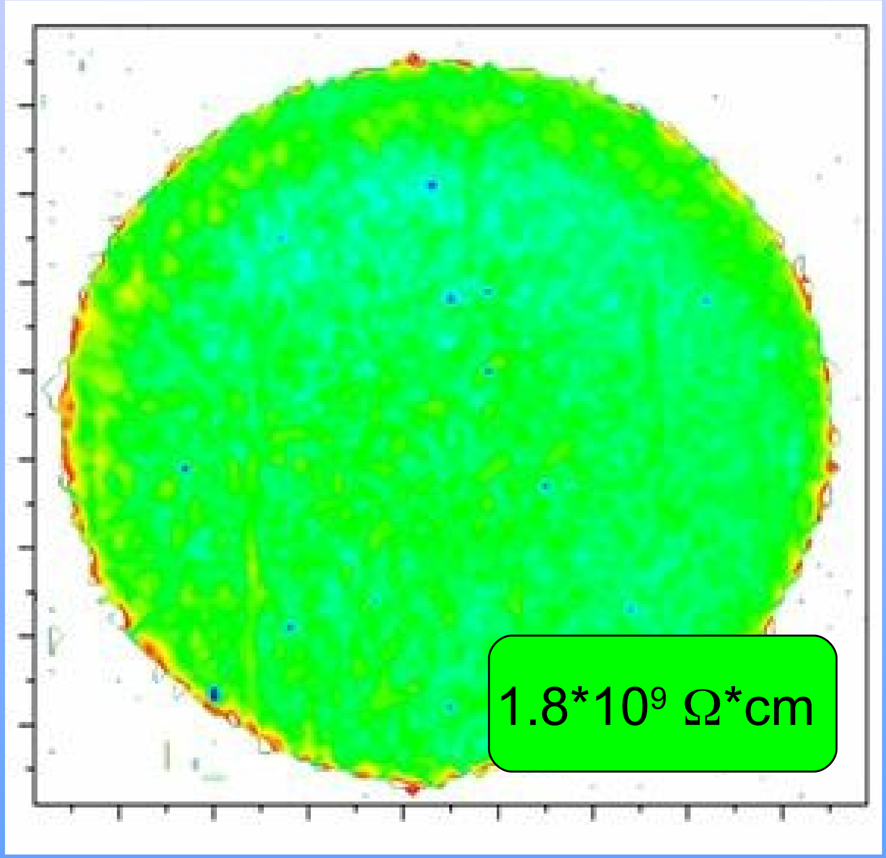

IV characteristics of Ni-HR GaAs-Ni pad sensors

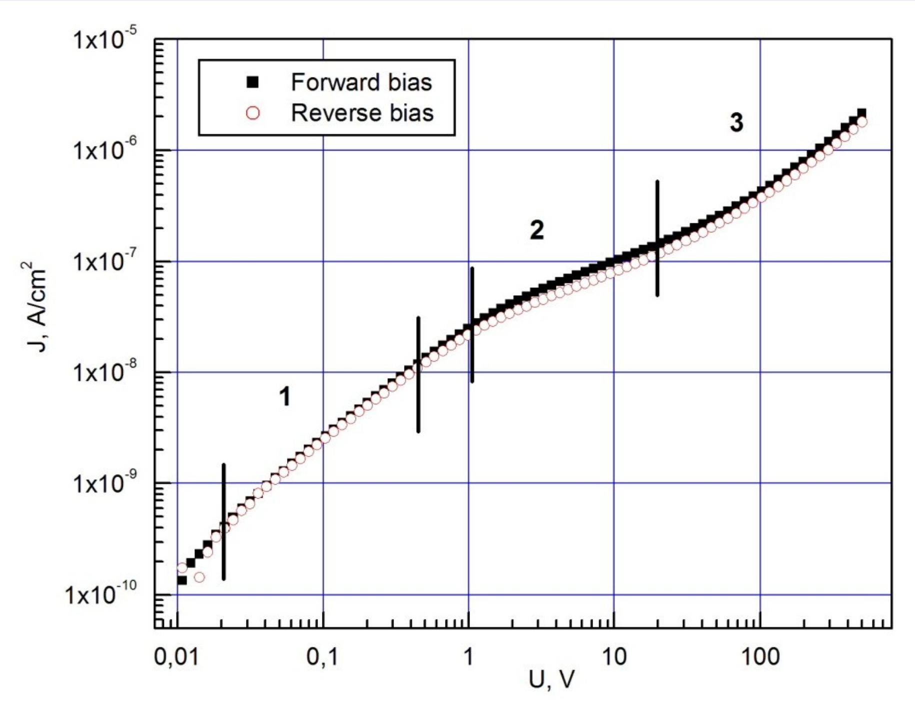

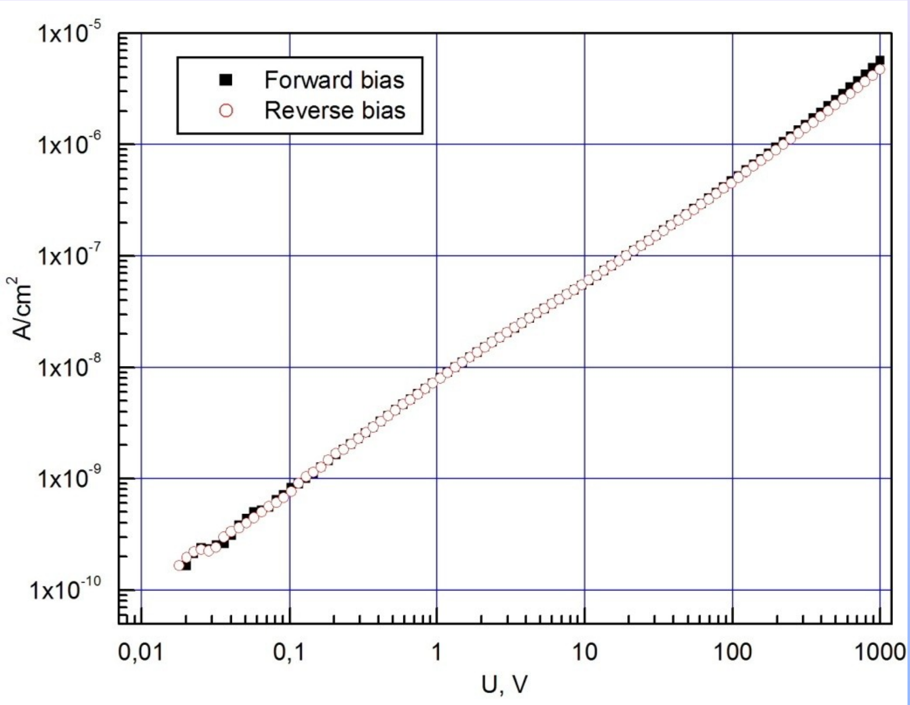

500 um thickness

980 um thickness

$$J \propto U^B$$

Section 1 (from 0.02 to 0.5 V), section 2 (from 1 to 15 V, B ≈ 0.7 – 0.9) and section 3 (>20 V, B ≈ 1.1 – 1.3)

Pulse height distribution for pad GaAs:Cr sensors, ^{241} Am source

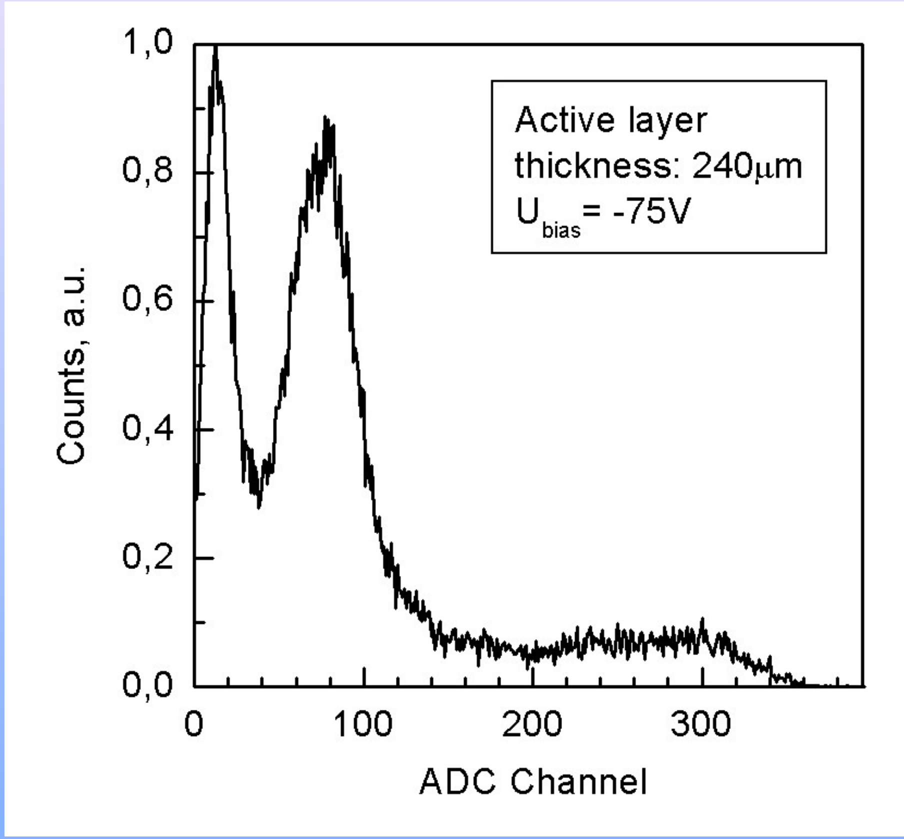

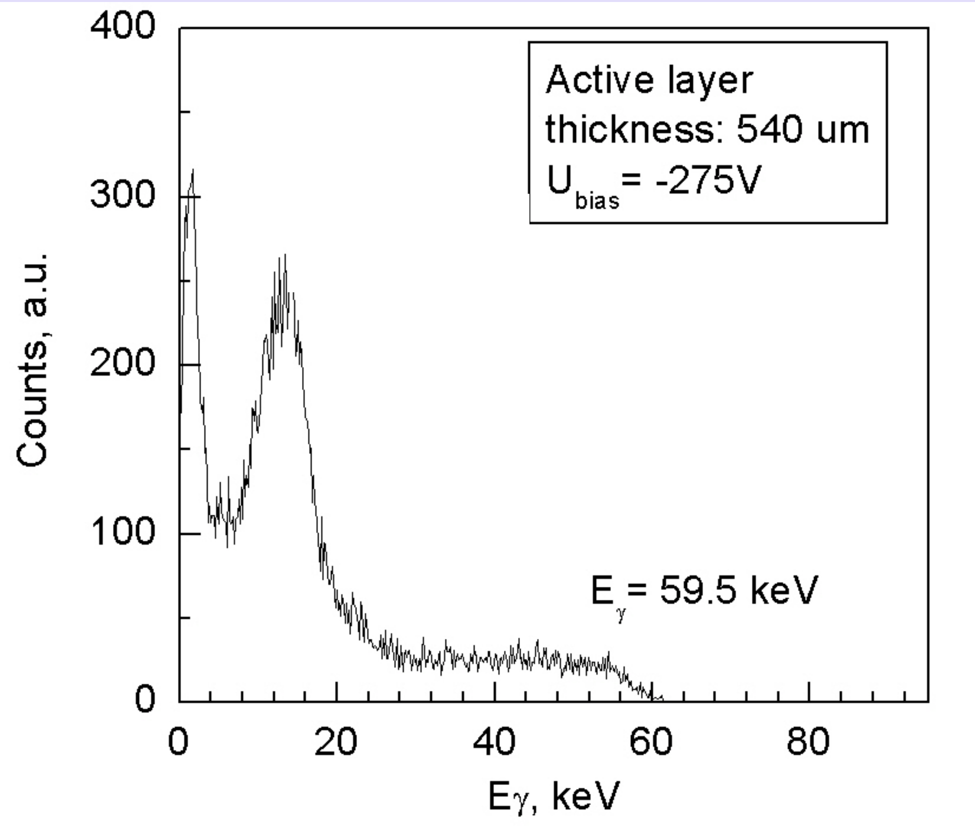

Unipolar charge collection - electrons

Charge collection efficiency of HR GaAs sensors

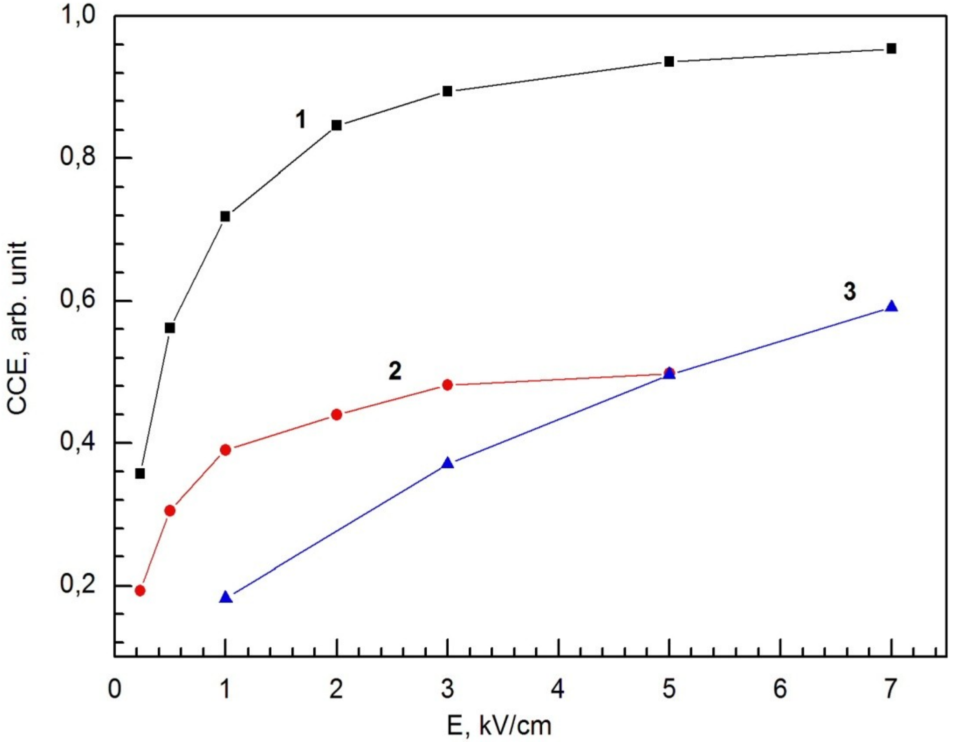

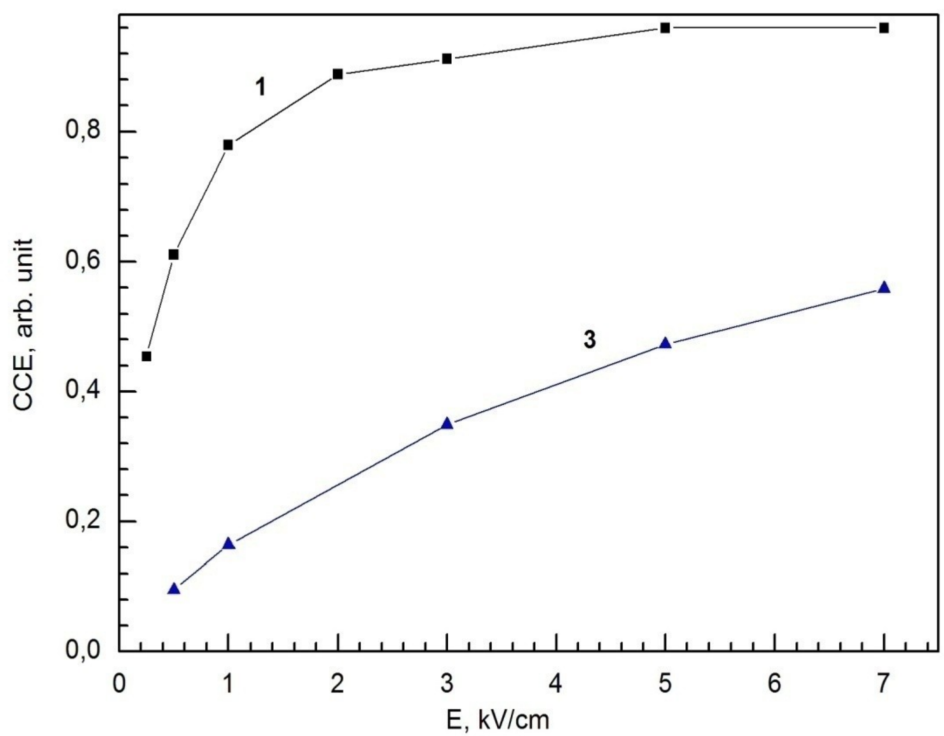

520 um thick pad sensor

1000 um thick pad sensor

1 - 60 keV gamma quanta, **3** - 5.6 MeV alpha-particles ^{241}Am source;

2 - 1 MeV beta-particles, ^{90}Sr source

Values of mobility * lifetime products

$\mu \cdot \tau$	CCE_{α}	CCE_{β}	CCE_{γ}
$(\mu \cdot \tau)_n$, cm^2/V	$6.8 \cdot 10^{-6}$	$6.0 \cdot 10^{-5}$	$7.6 \cdot 10^{-5}$
$(\mu \cdot \tau)_p$, cm^2/V	-	$3.0 \cdot 10^{-7}$	-

X-ray sensitivity dependence on bias

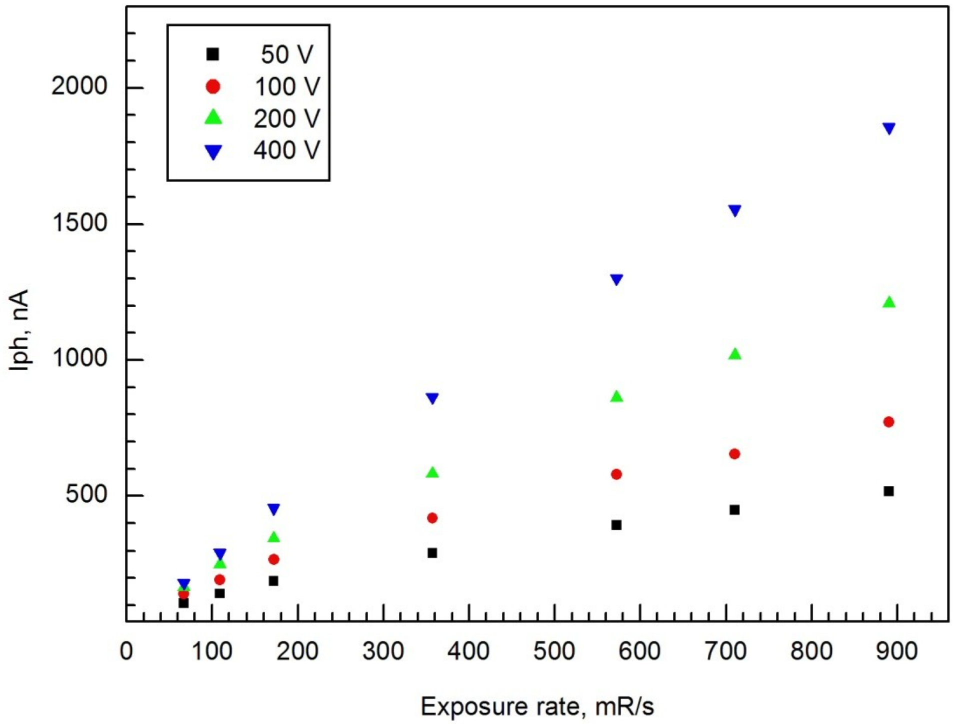

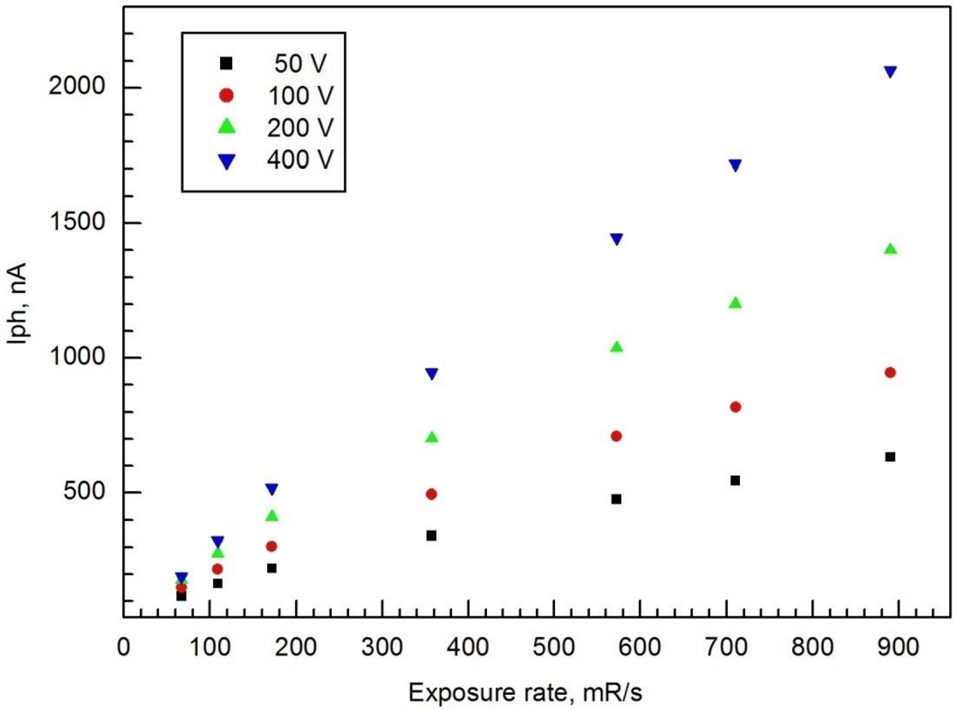

Anode irradiation

Cathode irradiation

W anode X-ray tube, 4 mm Al filter, 80kVp. 500 um thick HR GaAs pad X-ray sensors

HR GaAs pixel sensors

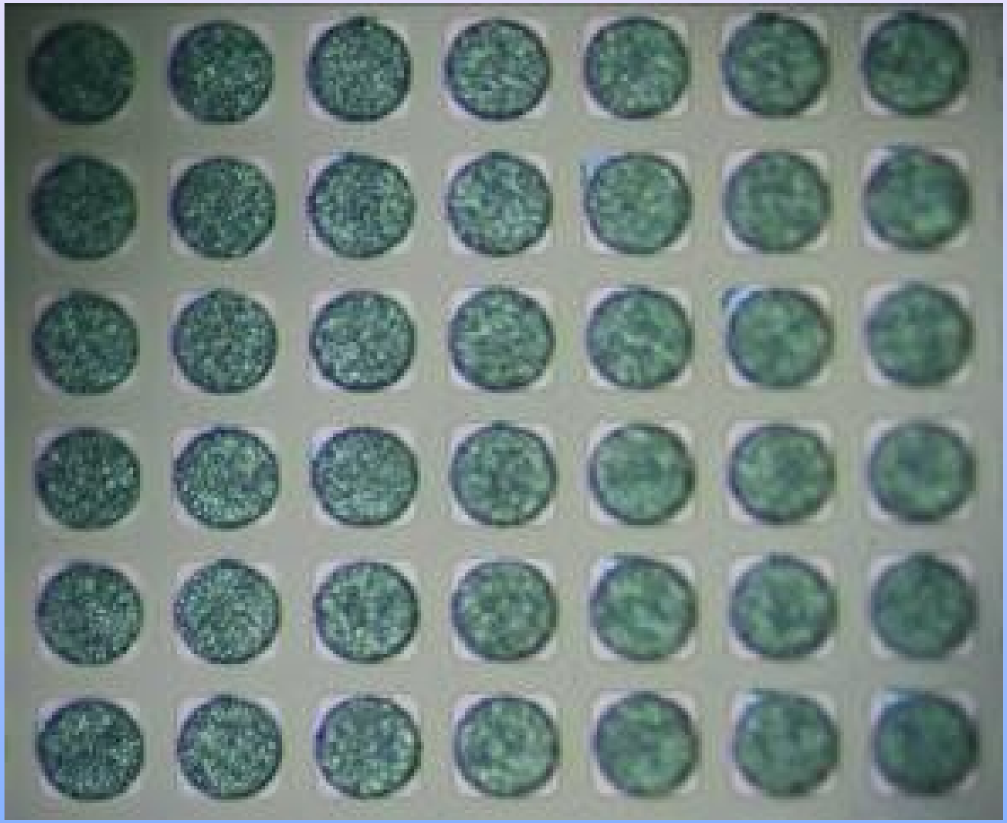

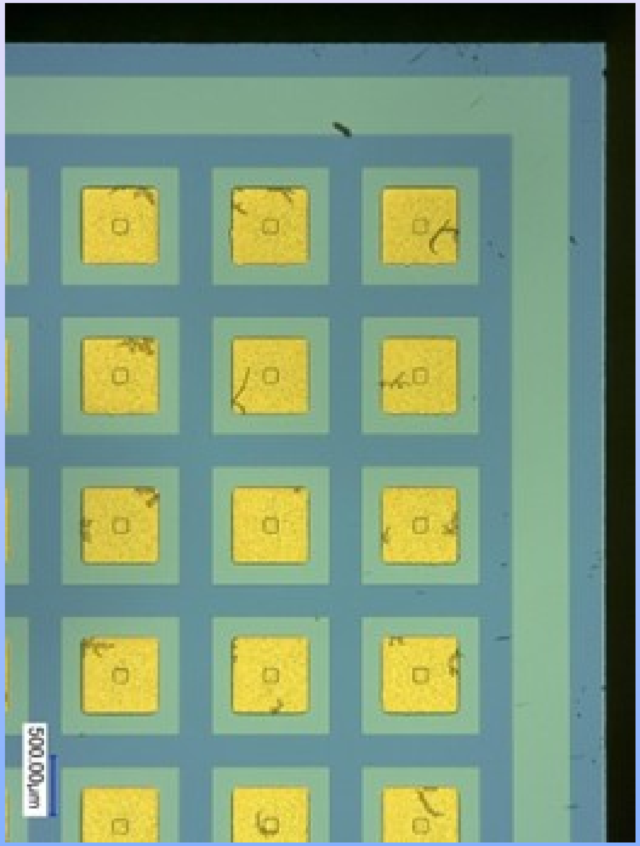

Pixel dimension: 45*45 um², number of pixels: 256*256, 768*512, and 55um pitch

Pixel dimension: 200*200 um², number of pixels: 80*80, and 250um pitch

Images obtained with a 512×768 HR GaAs Timepix ASIC pixel detector

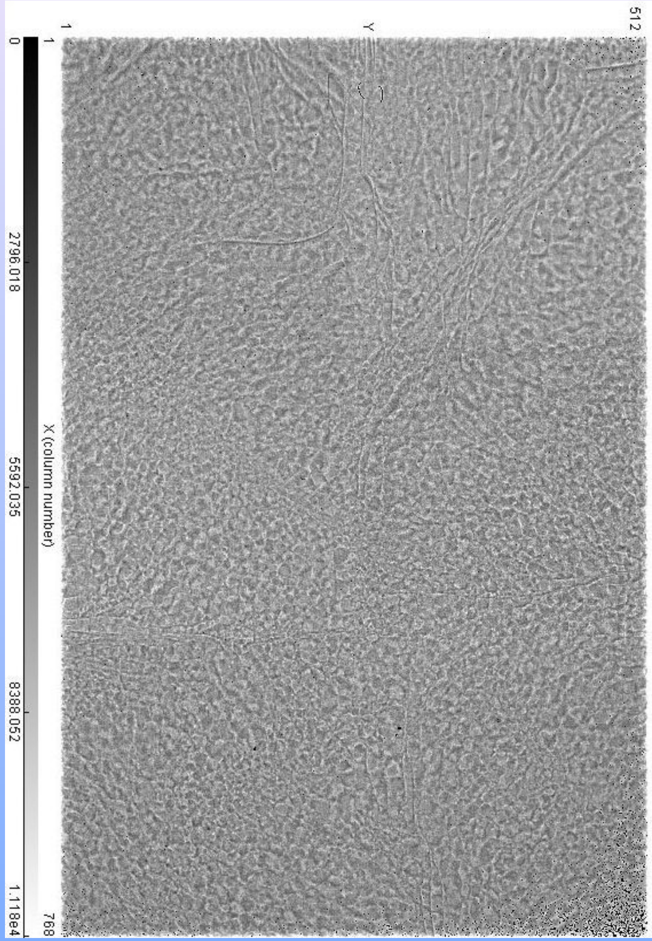

Uniform X-ray irradiation

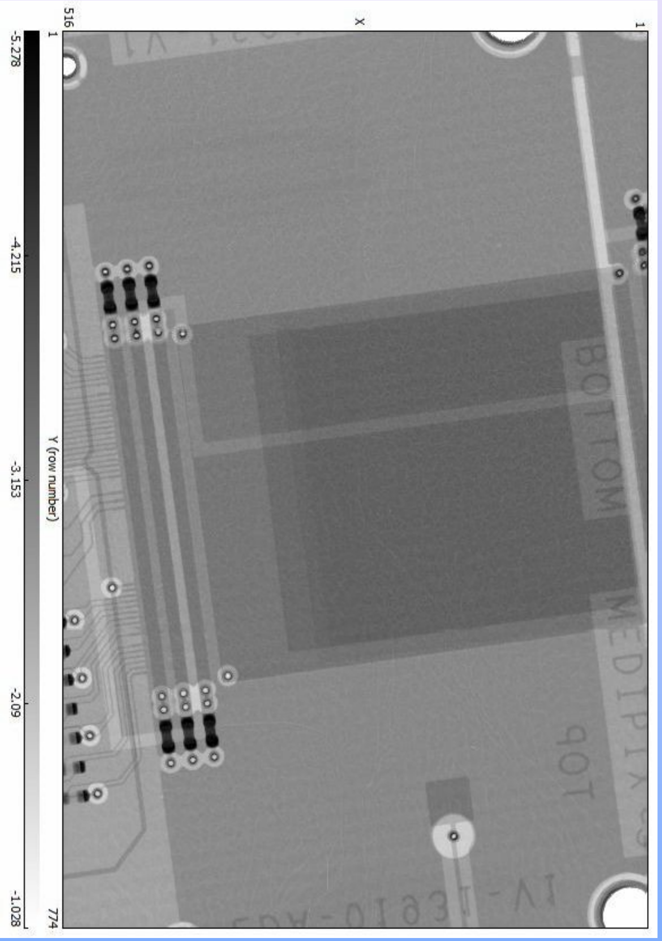

Image of test object

Procured by S. Procz (FMF, Albert-Ludwigs-University Freiburg, Germany)

Images obtained with a 256×256 HR GaAs Timepix ASIC pixel detector

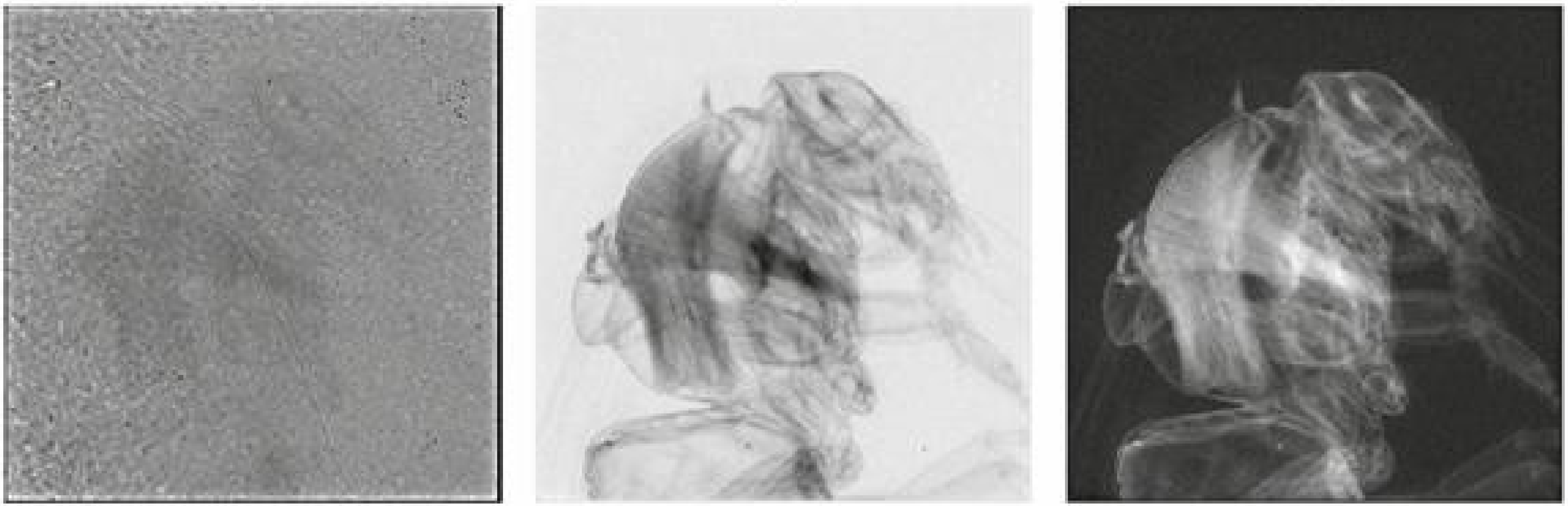

a b c

a): Raw image of a bumblebee acquired at 40 kVp and 500 μA;

b) Flatfield corrected image from a);

c): Negative logarithm of the flatfield corrected image for contrast enhancement.

Procured by E. Hamann (IPS, Karlsruhe Institute of Technology, Germany)

Spatial resolution of 256×256 HR GaAs Timepix ASIC pixel detector

Image of a lead ‘besom test’ pattern

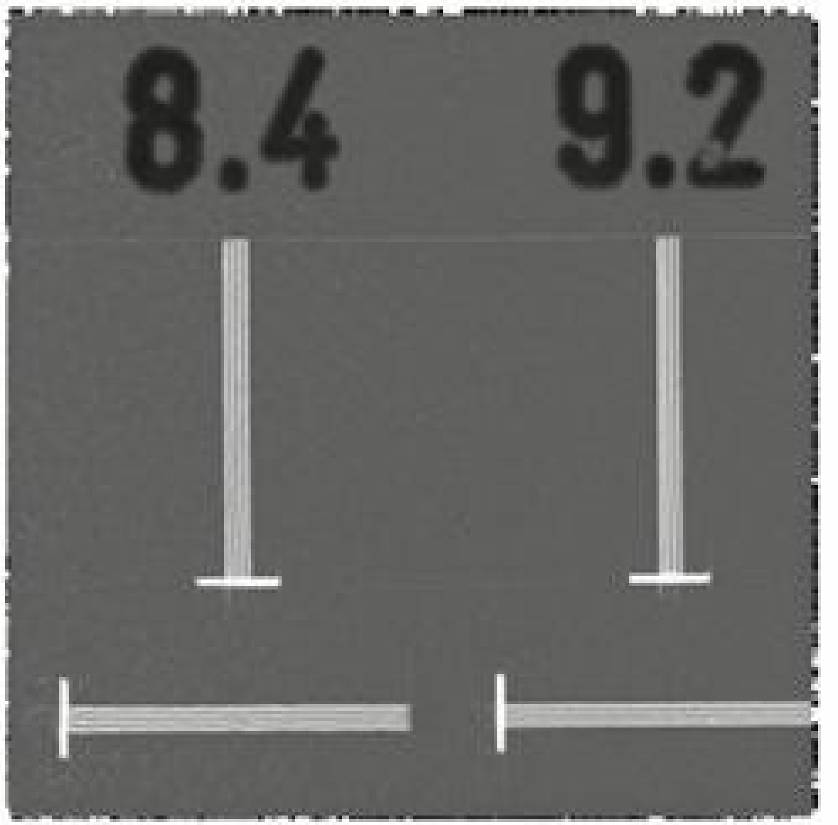

Image of a line pair pattern. The numbers indicate spatial frequencies in mm^{-1}

Procured by E. Hamann (IPS, Karlsruhe Institute of Technology, Germany)

X-ray images of test objects

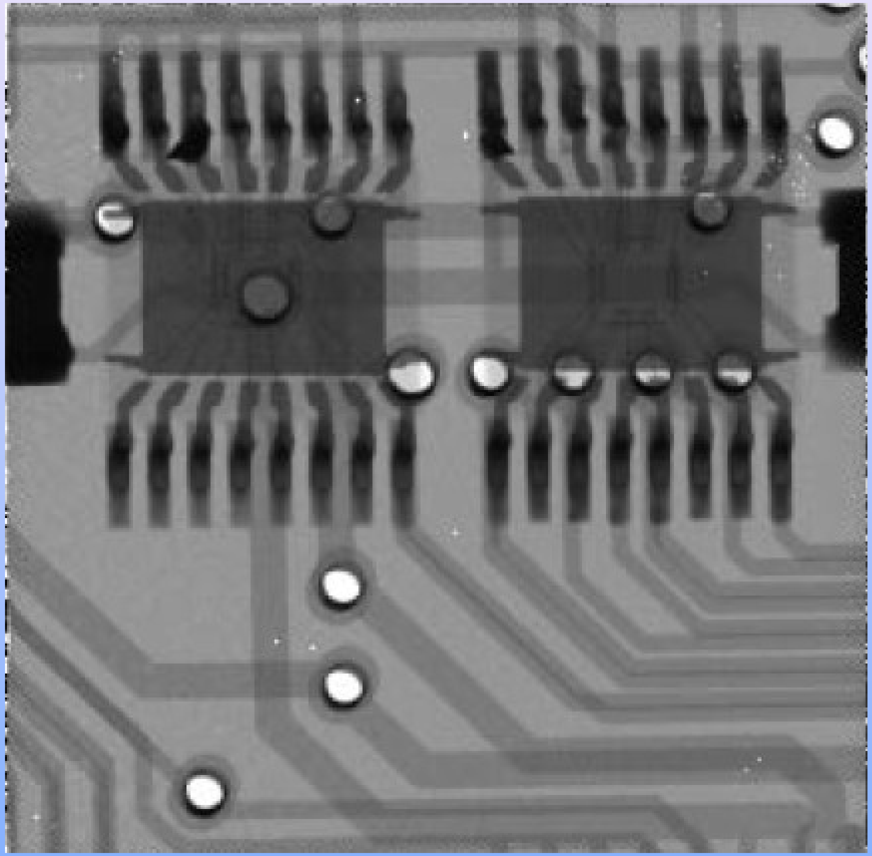

Flatfield corrected X-ray image of an integrated circuit on a PCB[1]

Flatfield corrected image of a lead test pattern for spatial resolution tests [1]

1- http://iopscience.iop.org/1742-6596/425/6/062015, E Hamann et al.

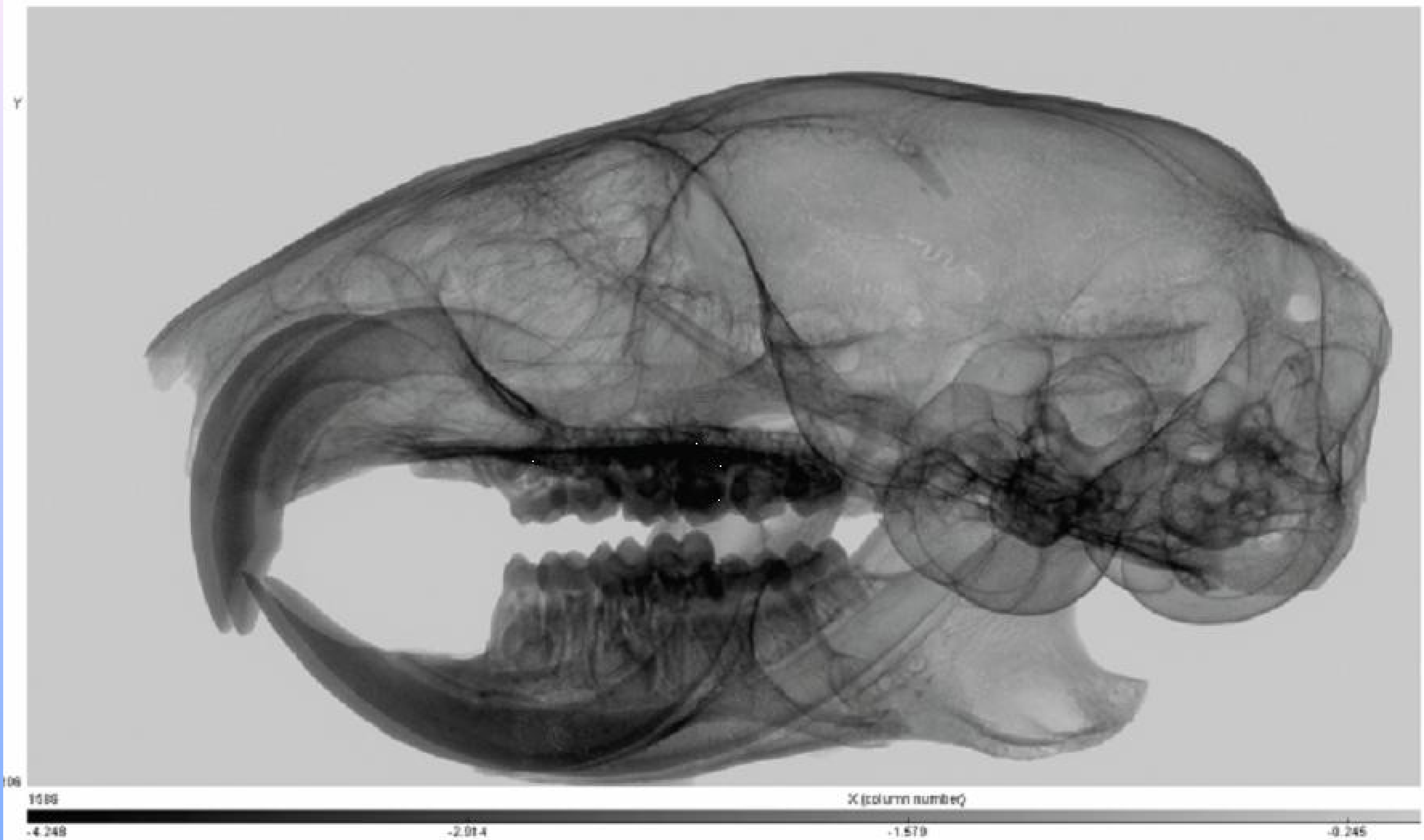

MPX3 assembly 25 kV – 200 V TH0 6 keV

Procured by Simon Procz, FMF, Albert-Ludwigs-University, Germany

MTF for all combinations of photon energies and threshold levels

Photon energy:	10 keV	15 keV	15 keV	25 keV	25 keV	25 keV
Threshold:	8.5 keV	8.5 keV	12 keV	8.5 keV	12 keV	15 keV
70% MTF	9 mm^{-1}	6.8 mm^{-1}	9.5 mm^{-1}	6.2 mm^{-1}	7.5 mm^{-1}	8.7 mm^{-1}
30% MTF	16.5 mm^{-1}	12.5 mm^{-1}	17.5 mm^{-1}	11.4 mm^{-1}	13.8 mm^{-1}	15.9 mm^{-1}
MTF @ $f_{Nyquist}$	69%	53%	72%	46%	59%	67%

Spatial frequencies at 70% and 30% MTF and MTF values at the Nyquist frequency for all combinations of photon energies and threshold levels

Procured by E. Hamann (IPS, Karlsruhe Institute of Technology, Germany)

Temperature stability of 256×256 HR GaAs Timepix ASIC pixel detector

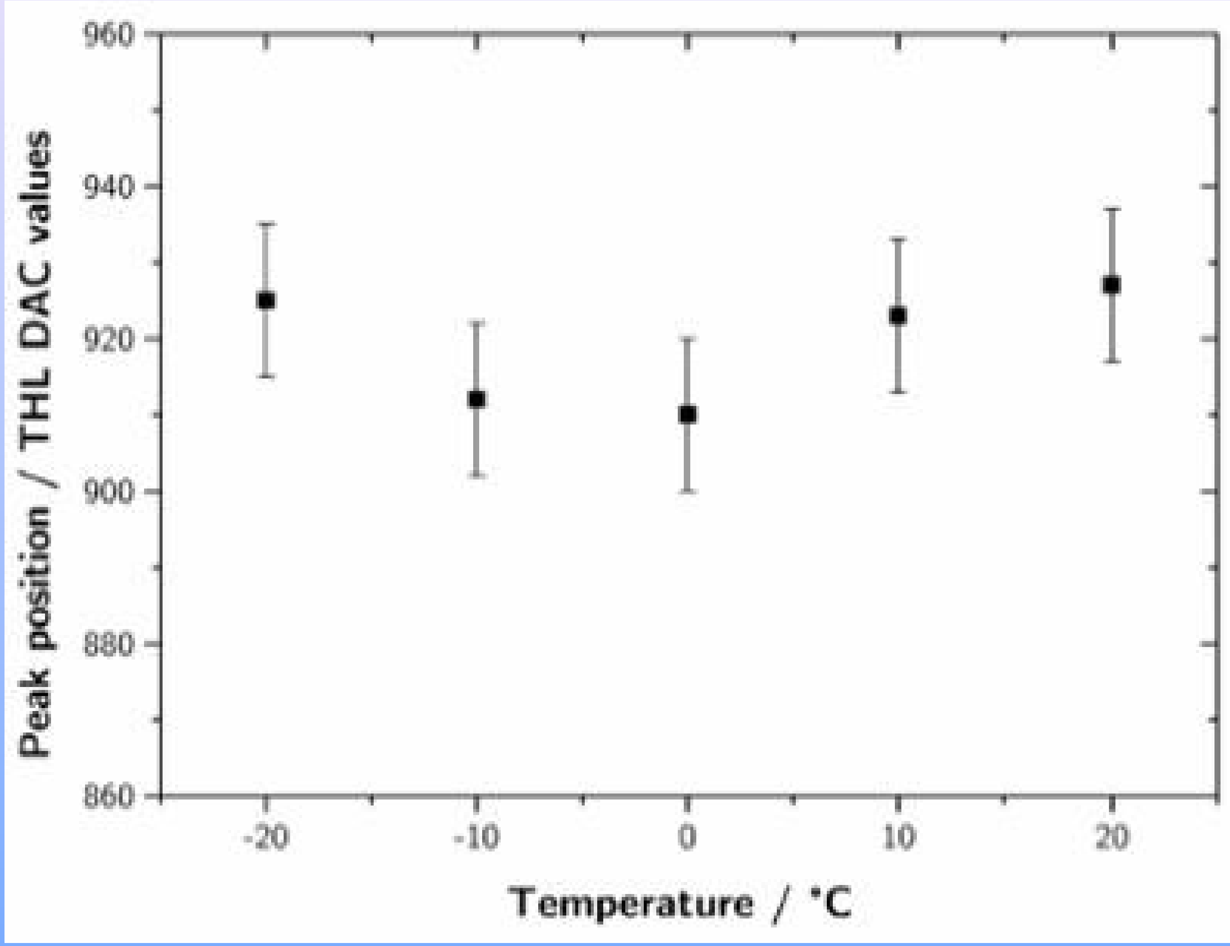

59.5 keV peak position under temperature variations from -20°C to +20°C.

Peak positions are stable and consistent within their errors.

Procured by E. Hamann (IPS, Karlsruhe Institute of Technology, Germany)

Active volume depth estimation of 256×256 HR GaAs Timepix ASIC pixel detector

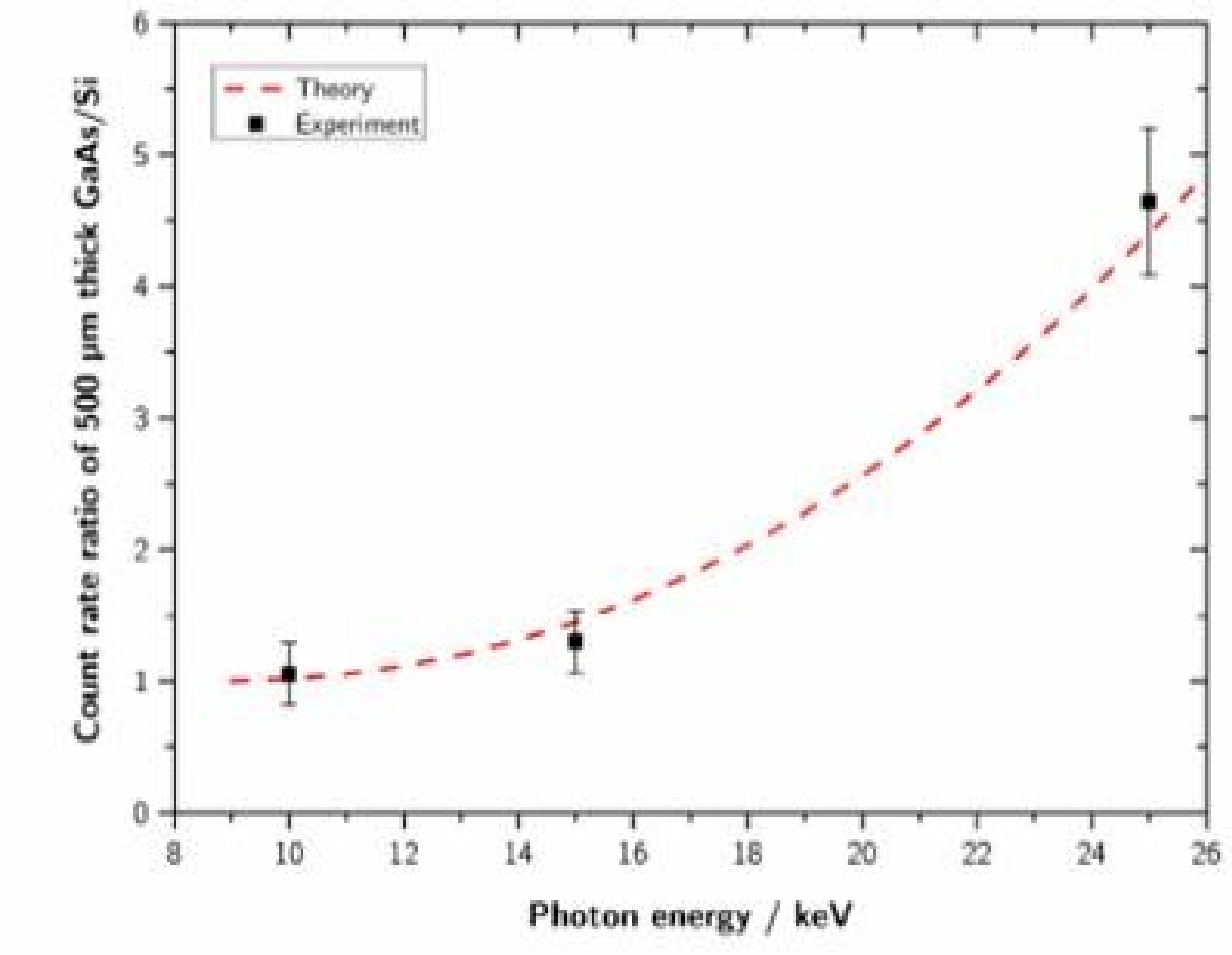

Experimental and theoretical ratios of count rates of 500 µm thick GaAs and Si sensors for several photon energies

Procured by E. Hamann (IPS, Karlsruhe Institute of Technology, Germany)

Distribution of the electric field strength in GaAs sensors

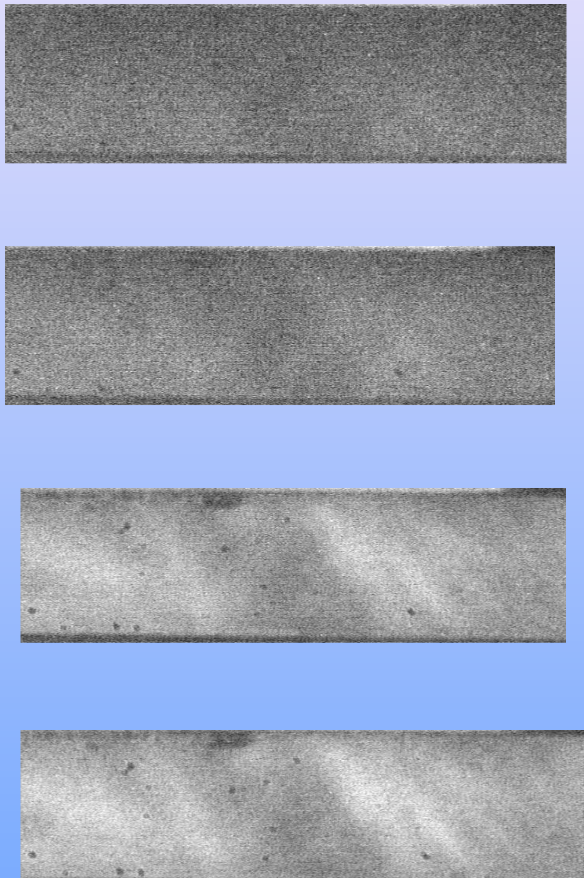

0 V

100 V

400 V

500 V

400 um thick HR
GaAs pad sensor

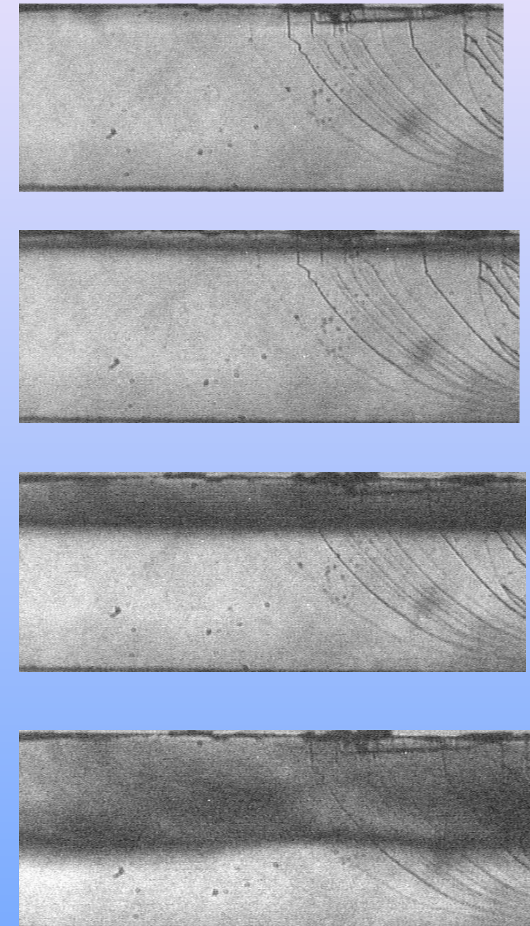

0 V

100 V

200 V

400 V

630 um thick “Schottky barrier -SI LEC
GaAs:EL2-ohmic contact“ sensor

Radiation resistance

gamma irradiation (E_g = 1.25 MeV)

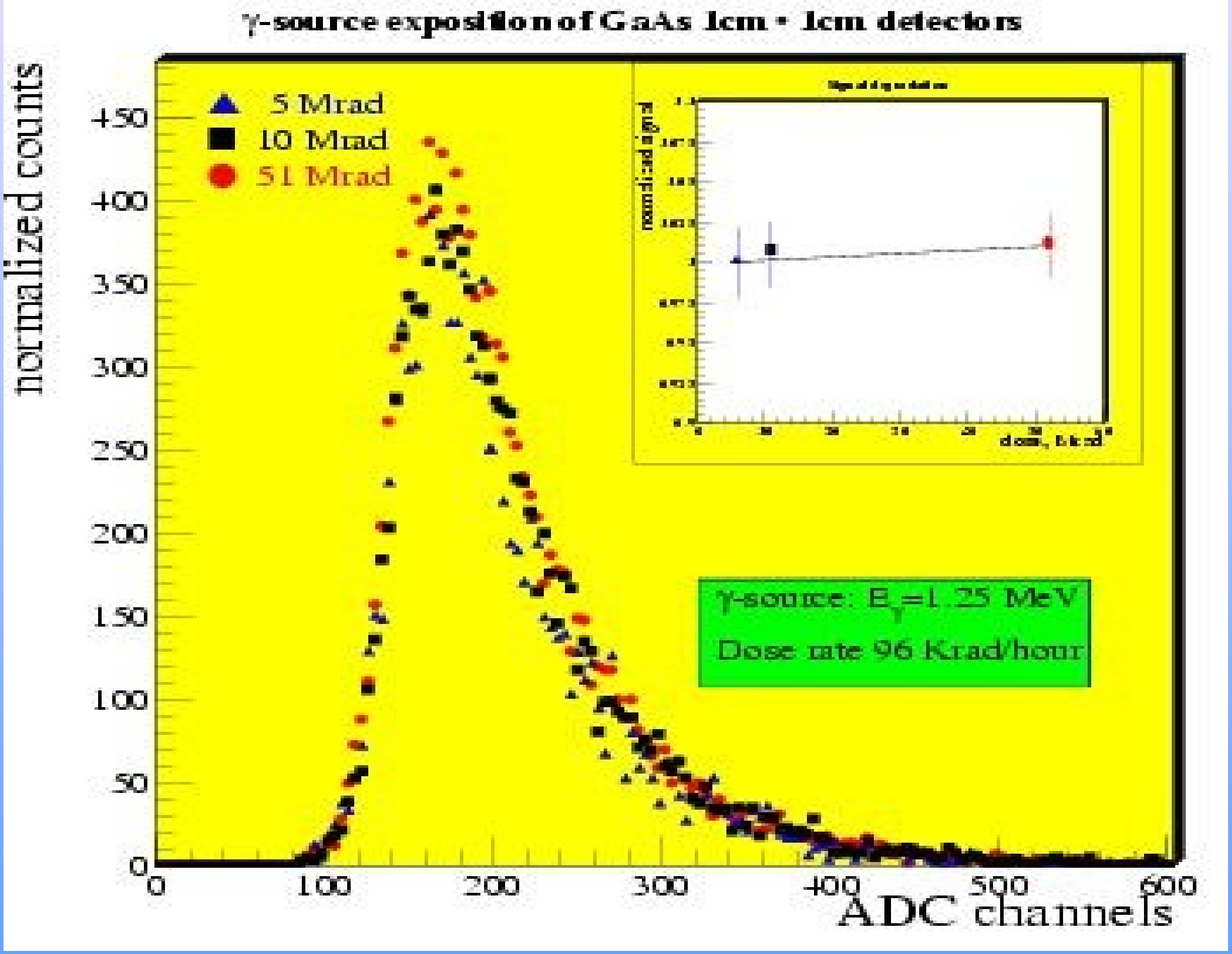

Radiation hardness

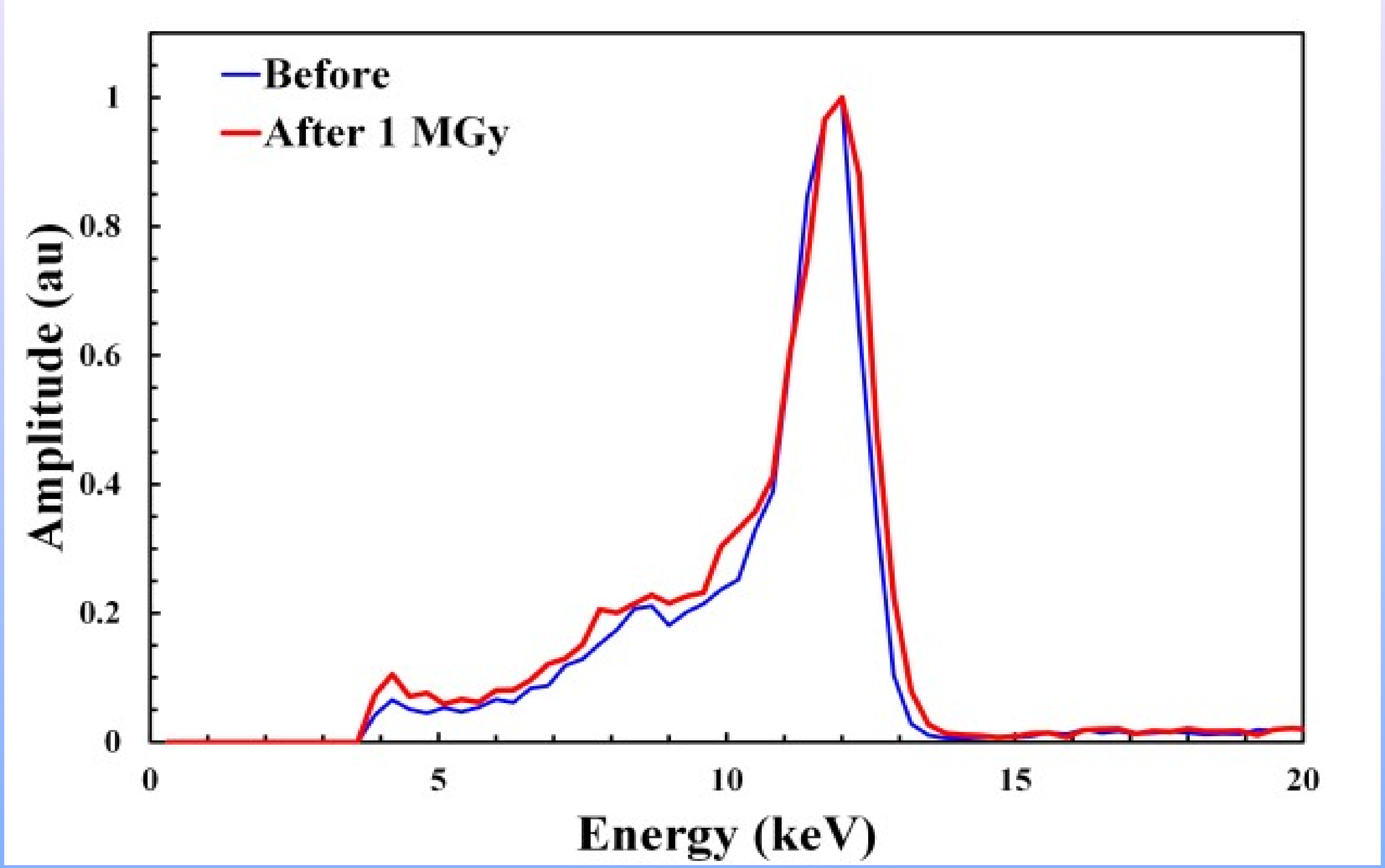

The spectrum of the 12 keV measured before and after a 1 MGy exposure, HR GaAs + HEXITEC ASIC detector

Procured by M. C. Veale et all. (RAL STFC, UK). Presented at IWORID 2014

Dependence of the count rate on the bias voltage

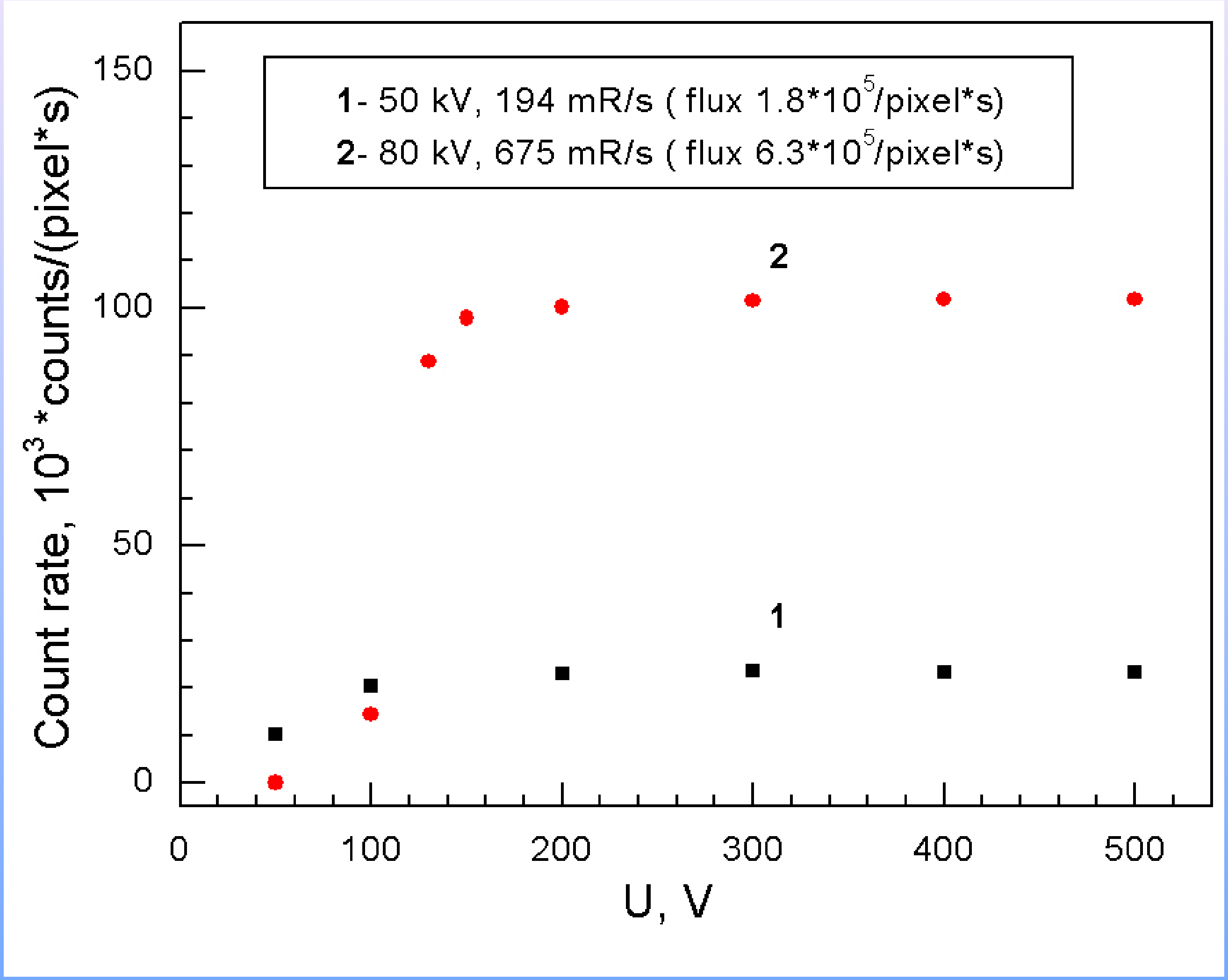

500µm GaAs:Cr +TPX detector @ X-ray tube voltage of 80kV

Maximal count rate

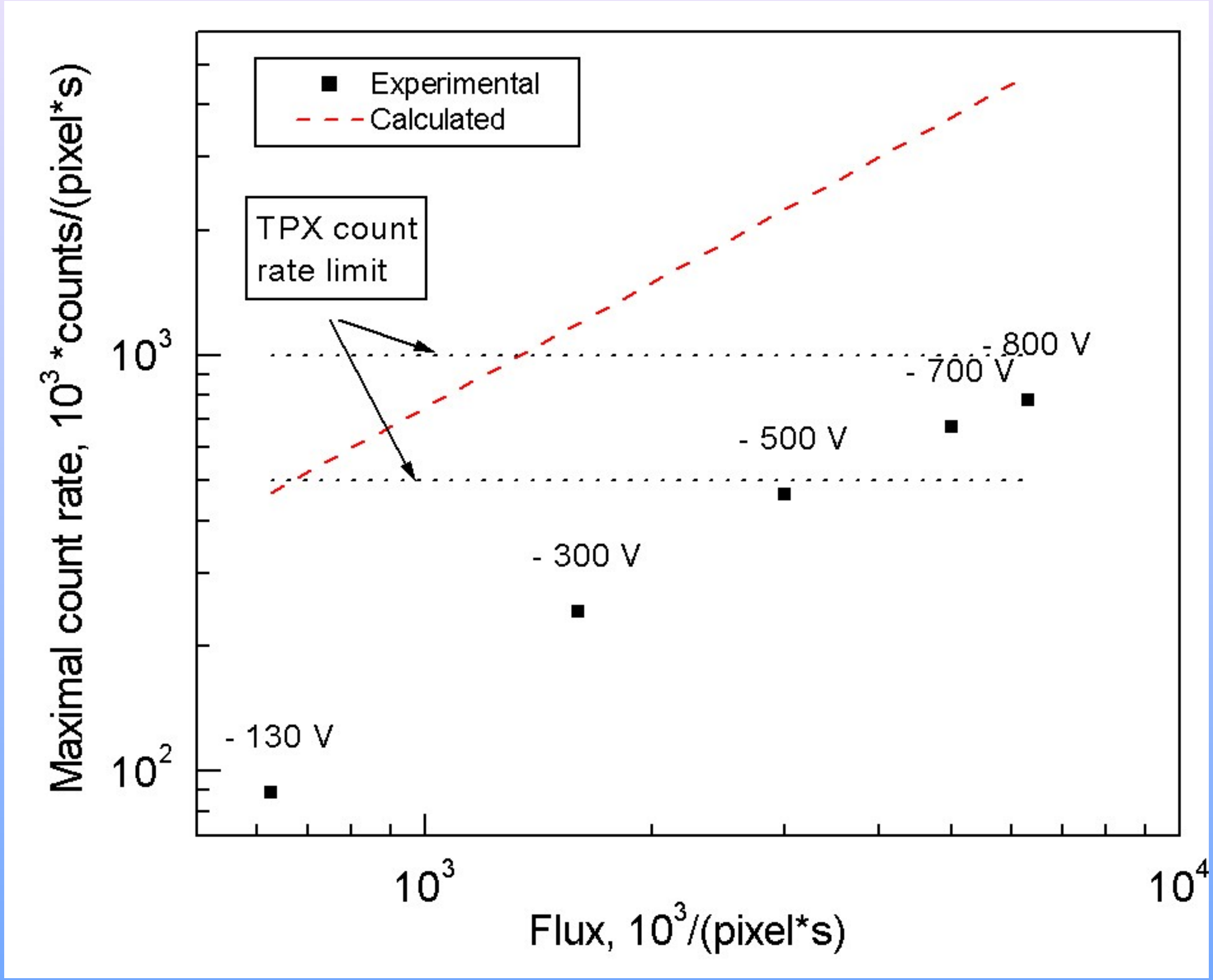

500µm GaAs:Cr +TPX detector @ X-ray tube voltage of 80kV

Stability of count rate under high flux

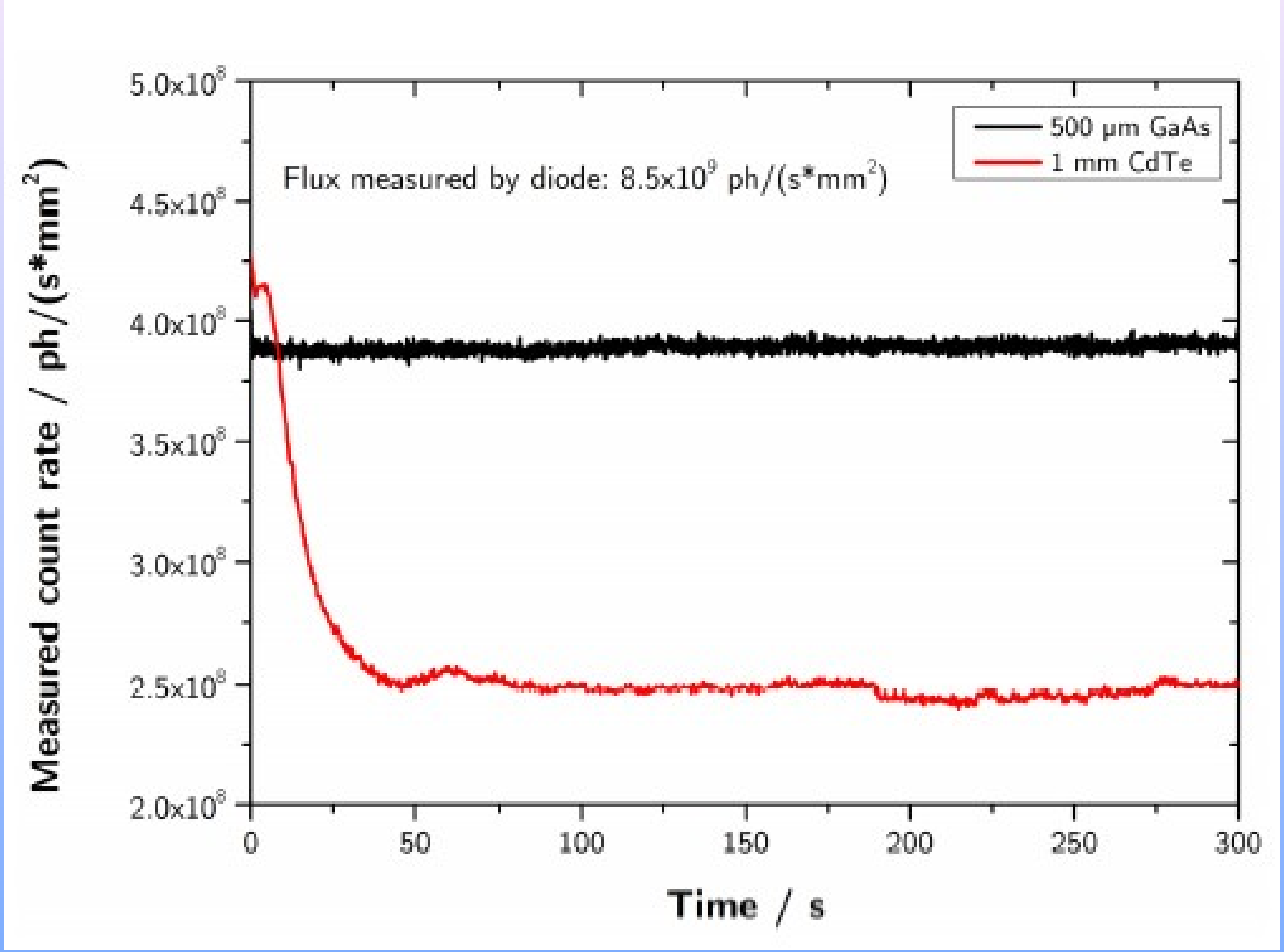

Count rate comparison of the 500 µm thick GaAs and the 1 mm thick CdTe assembly for a flux of 8.5*10⁹ ph/(s*mm²) of 16 keV X-ray

Procured by E. Hamann (IPS, Karlsruhe Institute of Technology, Germany)

Medipix3RX assembly with HR GaAs sensor

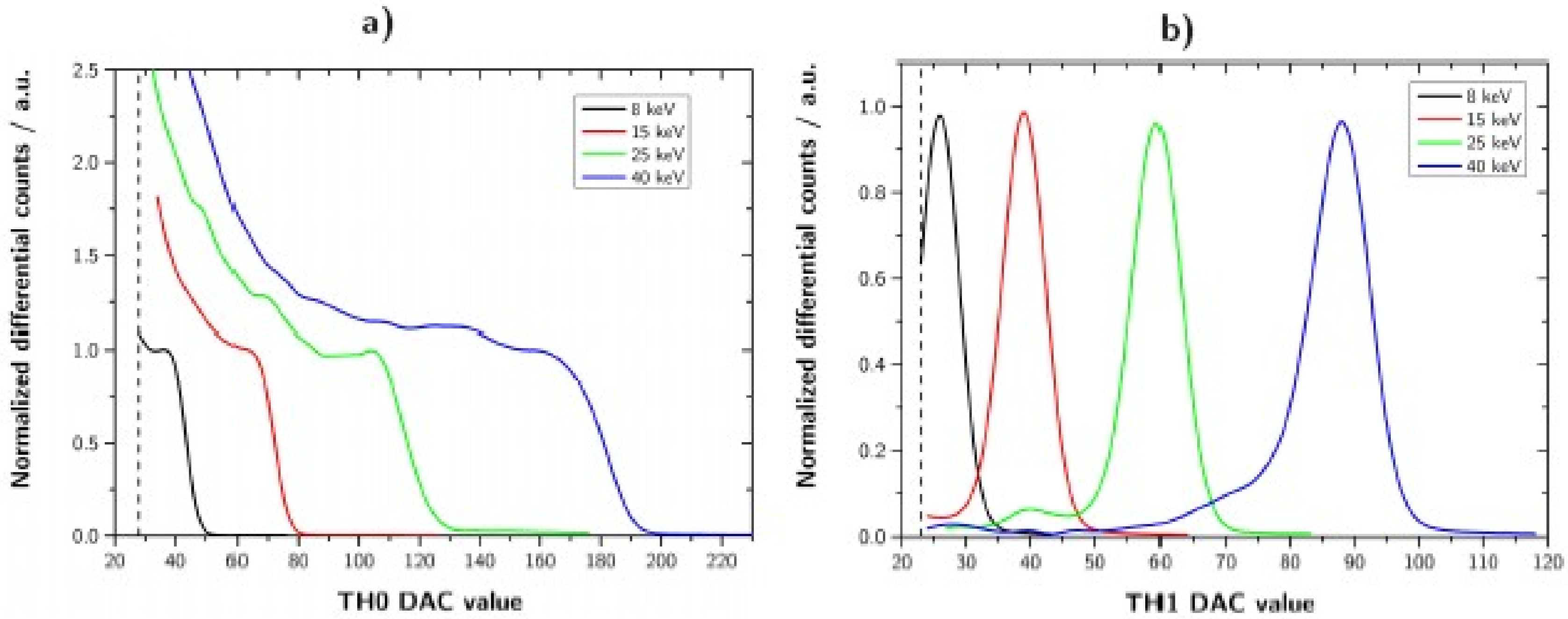

Figure 9.13: Normalized energy spectra in SPM (a) and in CSM (b) for monochromatic synchrotron radiation of 8 keV, 15 keV, 25 keV and 40 keV. The electronic noise level is indicated by the vertical dashed black line.

Normalized energy spectra in Charge Summing Mode (CSM) for monochromatic synchrotron radiation of 8 keV, 15 keV, 25 keV and 40 keV.

Procured by E. Hamann (IPS, Karlsruhe Institute of Technology, Germany)

Energy resolution HR GaAs pixel sensors

Table 9.1: Energy resolution (absolute and relative FWHM) of the CSM peaks for different photon energies as shown in Figure 9.13 b) and a Cd-109 source.

Photon energy / keV	8	15	22.5	25	40
FWHM / keV	2.8	3.4	4.34	4.16	4.5
FWHM / %	34.6	22.8	19.3	16.7	11.2

Procured by E. Hamann (IPS, Karlsruhe Institute of Technology, Germany)

The 500 um HR GaAs HEXITEC detector

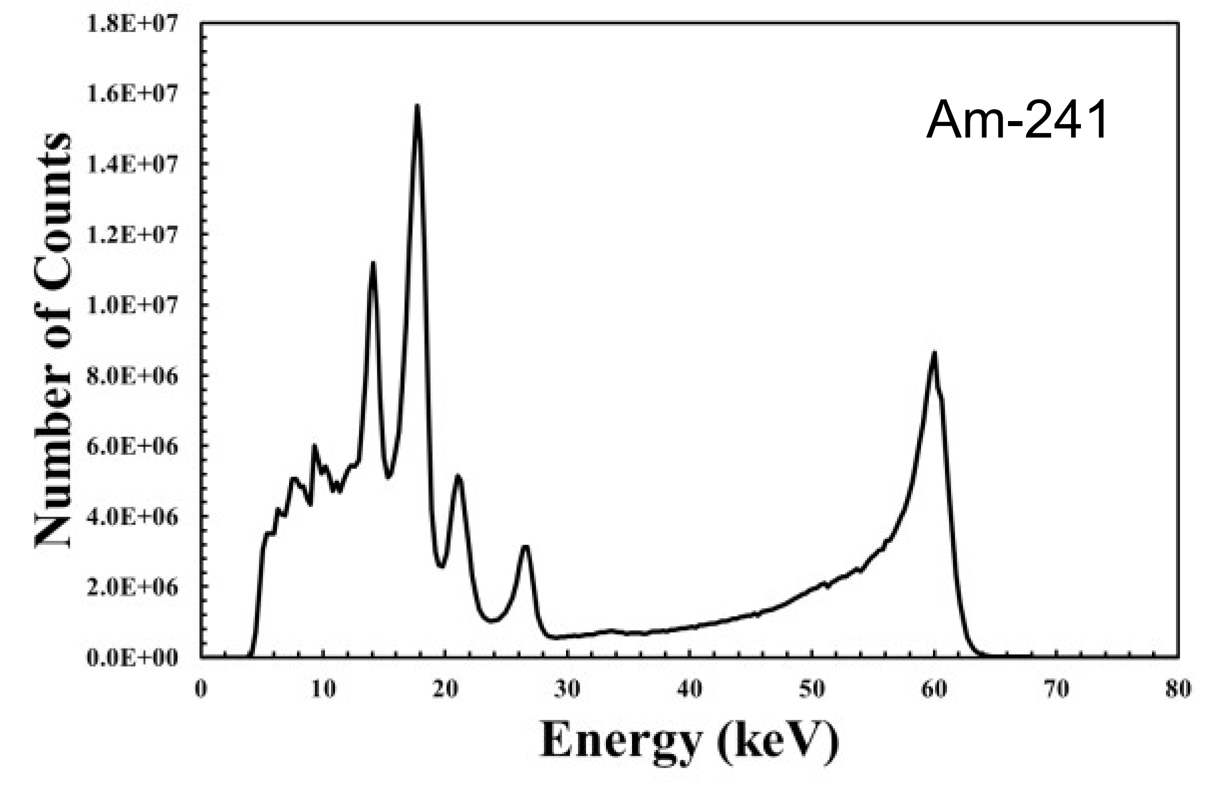

$FWHM_{@60keV}$ = 3.0 +/- 0.5 keV (10%)

Typical V_{bias} = 300 V

T = 7^0 C

Pixel dimension: 200*200 um^2

Procured by M. C. Veale et all. (RAL STFC, UK). Presented at IWORID 2014

Medipix3RX assembly with HR GaAs sensor

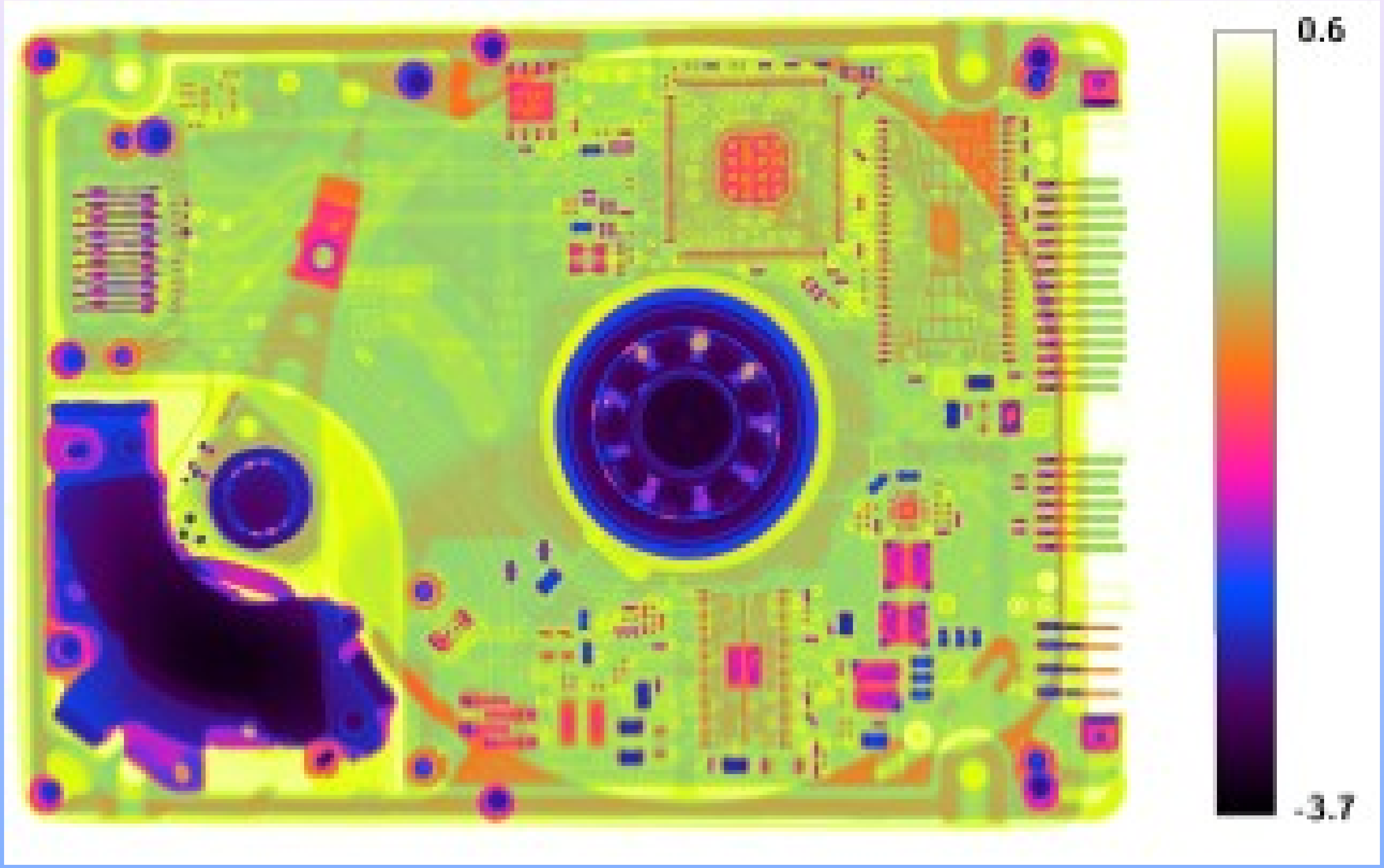

X-ray image of a computer hard drive recorded in SPM and the corresponding logarithmic pseudo-color bar. The image consists of 8×9 tiles recorded at a geometrical magnification of 1.05.

Procured by E. Hamann (IPS, Karlsruhe Institute of Technology, Germany)

Microtomography 3D movie

Obtained by G. Shelkov (JINR, Dubna, Russia)

Microtomography 3D images of bone

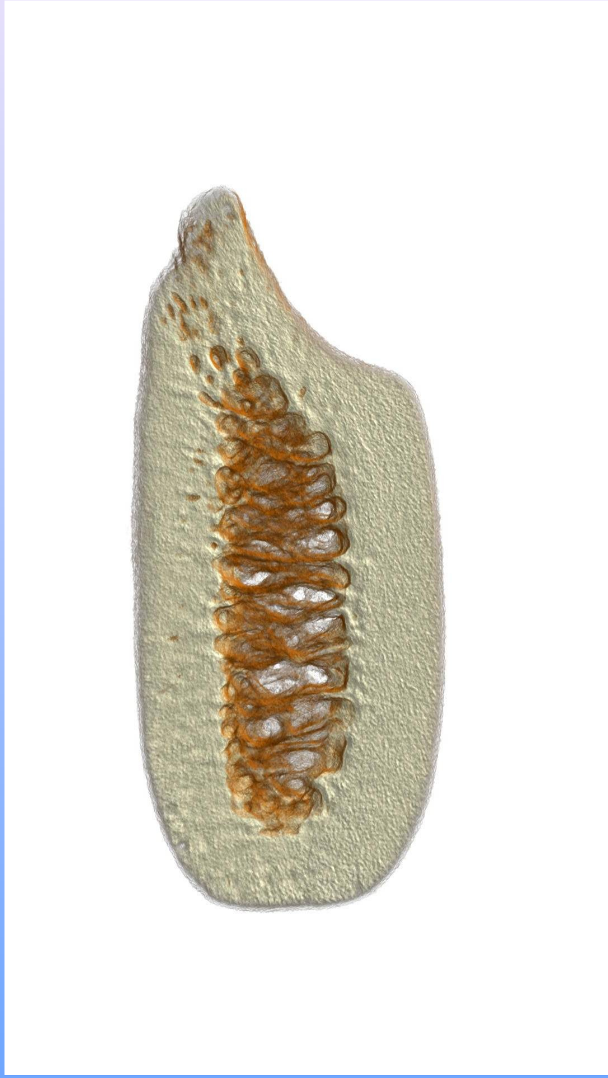

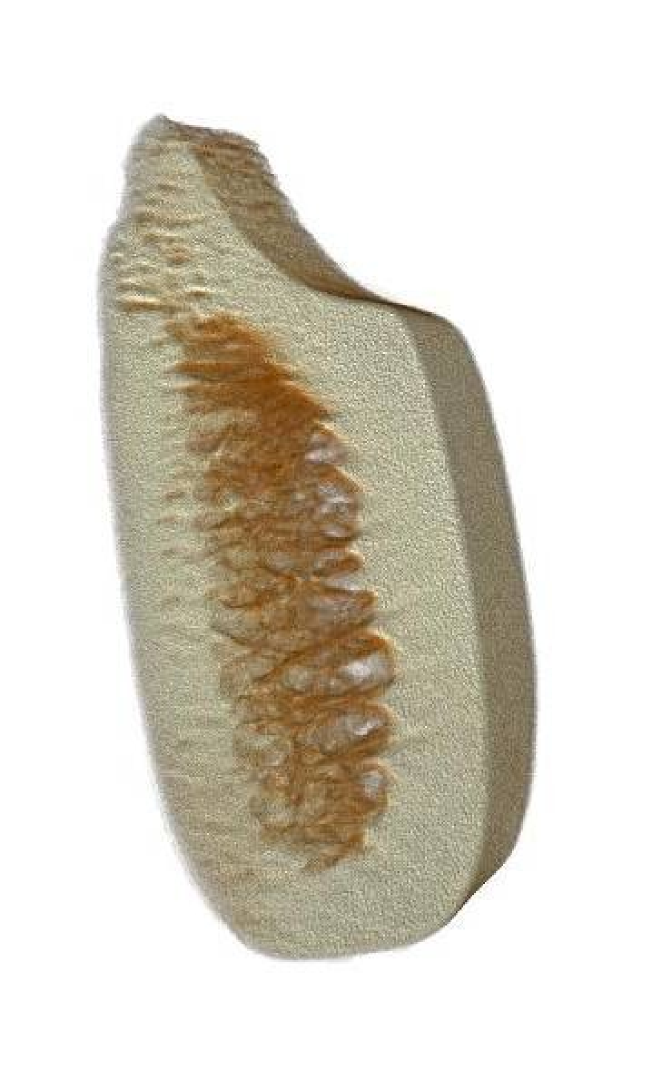

Obtained by G. Shelkov (JINR, Dubna, Russia)

Microstrip sensors

Pitch, μm	Number of channels	Chip dimension, mm^2	Active layer thickness, μm
400	64	4×25.6	
200	128	4×25.6	up to 1000
200	128	9×25.6	
100	256	4×25.6	
50	512	4×25.6	
100	512	51.2×51.2	
1200	32	15×38.4	

Pixel sensors

Pixel dimension μm^2	Number of pixels	Chip dimension, mm^2	Active layer thickness, μm
170×170	64×64	10.9×10.9	
55×55	256×256, 768*512	12.8×12.8	up to 1000
50×50	128×128	6.4×6.4	

HR GaAs strip sensor array & read-out electronic

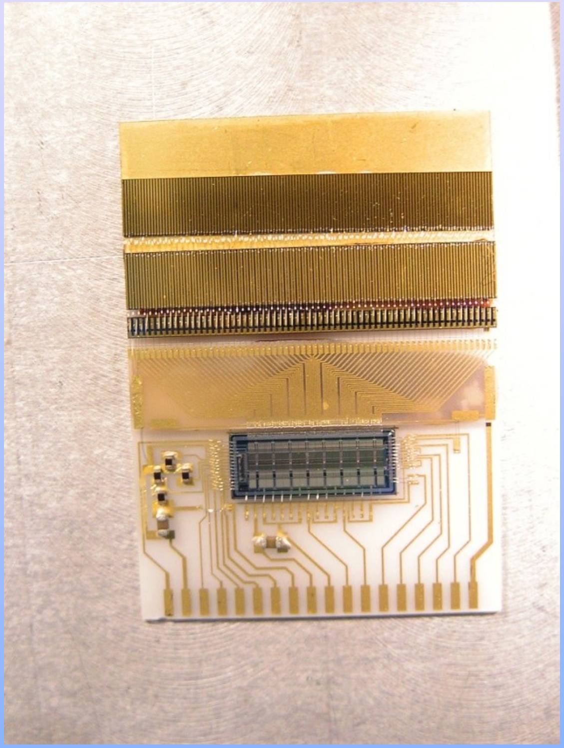

64 channels,
400μm pitch.
Quantum count
mode chip.

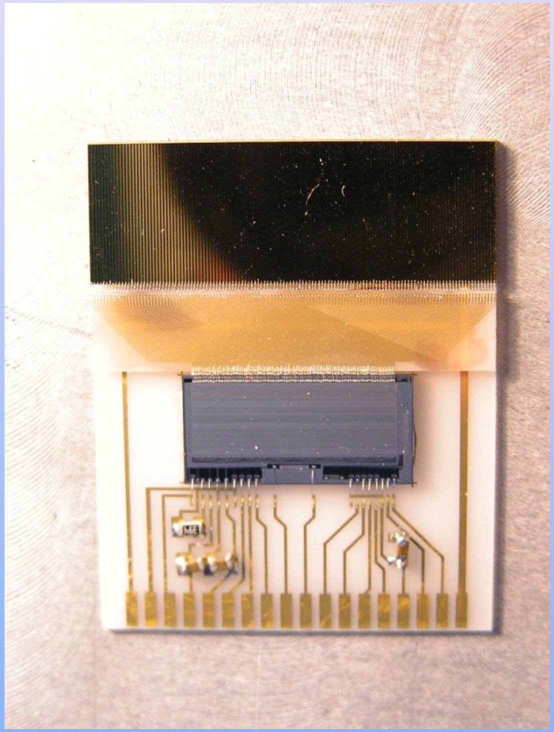

128 channels,
200μm pitch.
Integrating mode
chip.

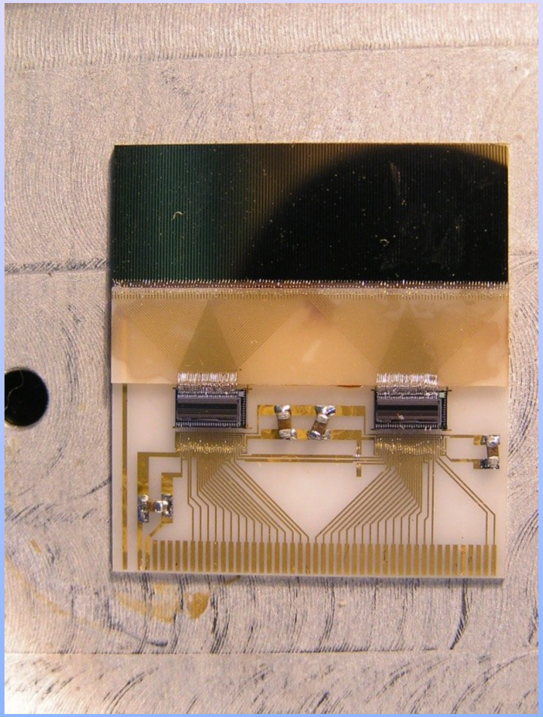

2*64 channels,
200μm pitch.
Integrating mode
chip.

LDA prototype for nondestructive testing

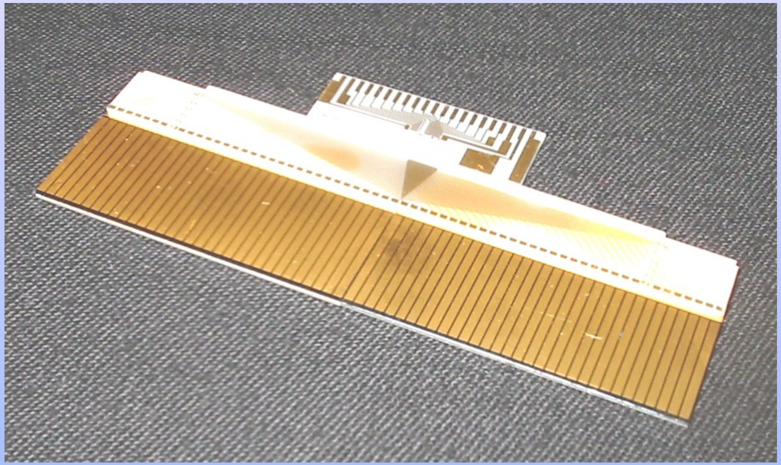

Detector module
Sensor pitch: 1.2 mm

The LDA operates in the pulsed mode with external triggering.
Total detector length: 538 mm

Detector module

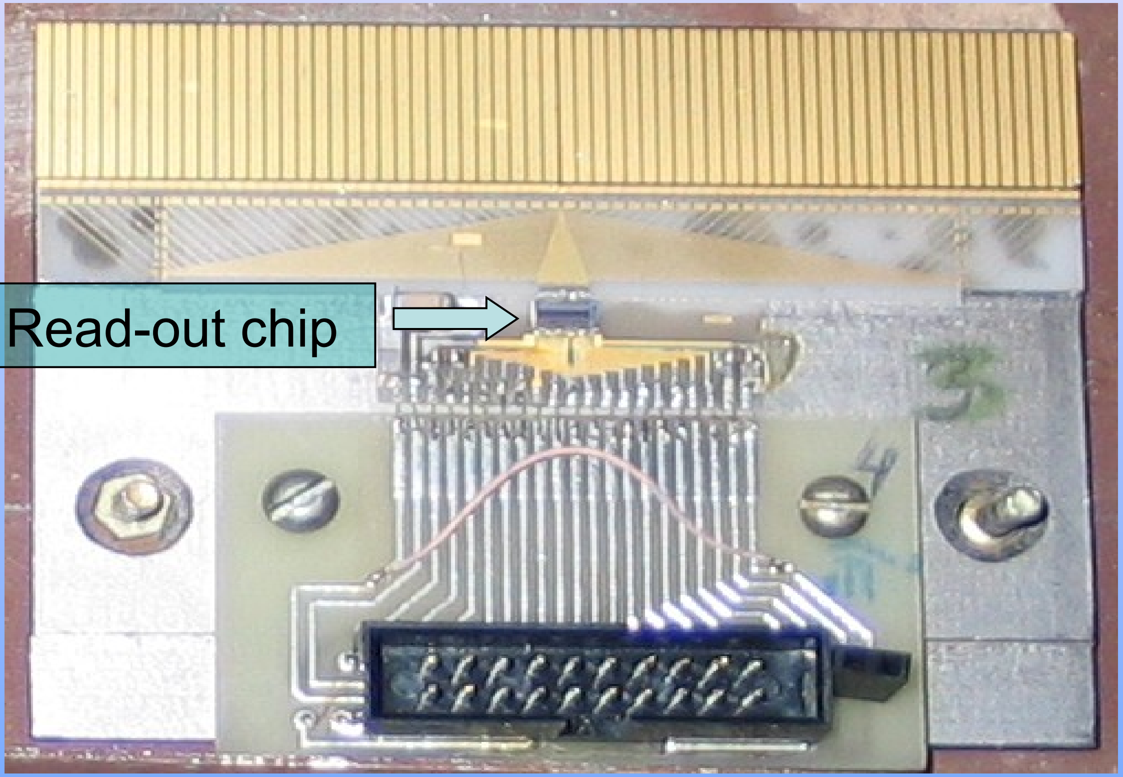

Detector module

51.2*51.2mm^2 GaAs strip sensor on ceramic substrate, 512 channels, 100um pitch

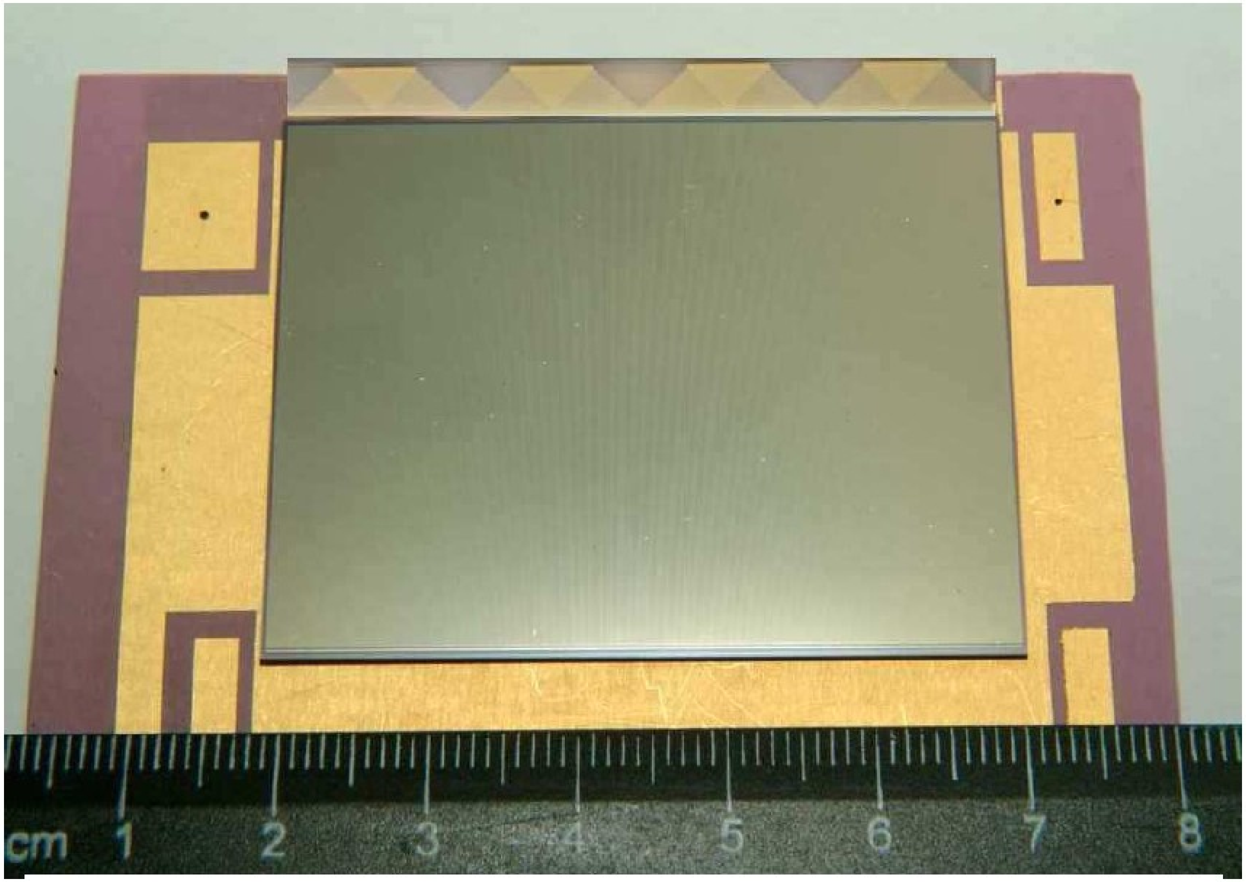

512 channels GaAs microstrip detector on ceramic carriers and fan-out for read-out chips

HR GaAs detector for R&D in field of high energy and nuclear physics

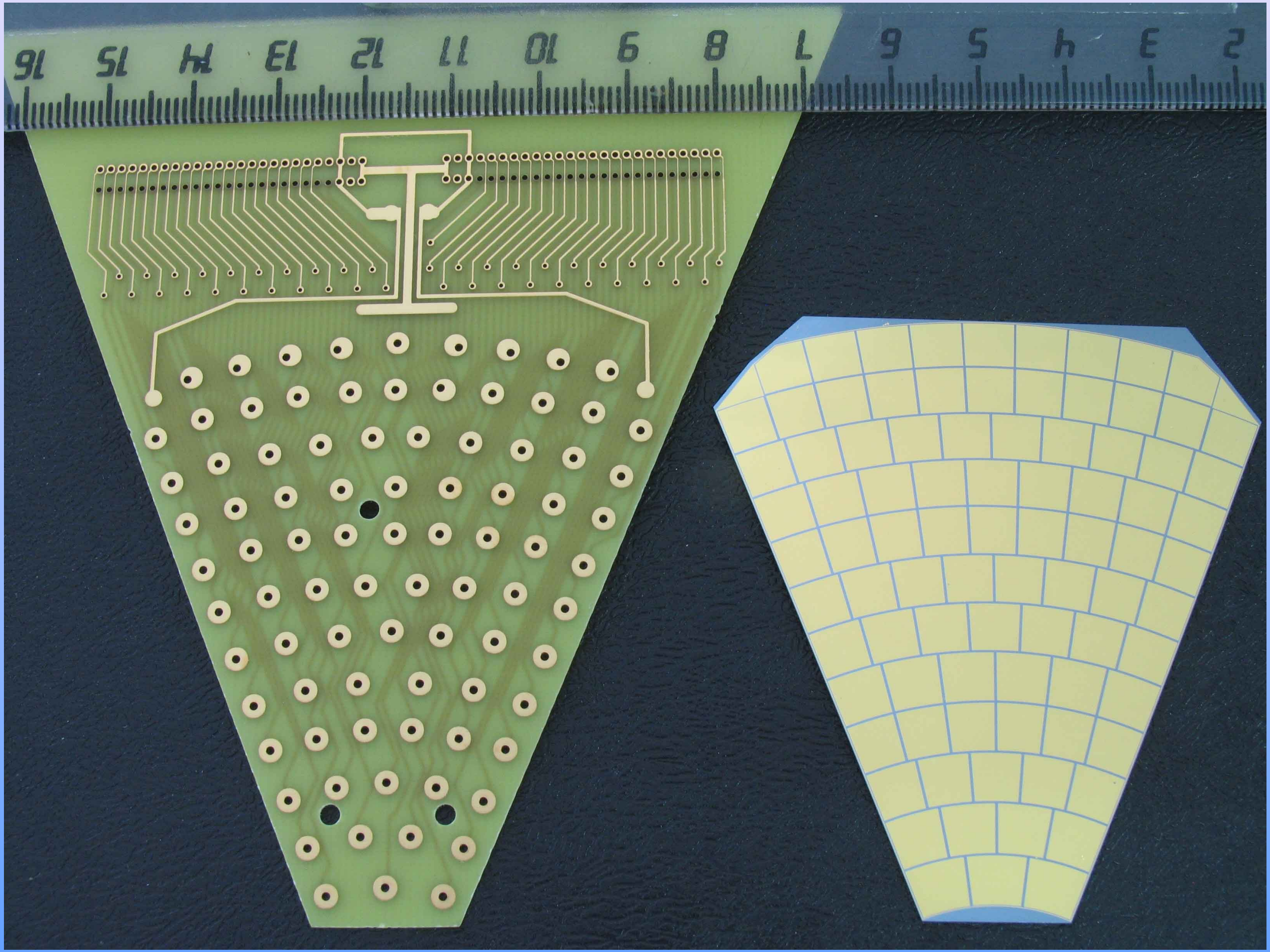

Conclusion

It has been shown that the technology of n-GaAs compensation with chromium enables to reach the HR GaAs resistivity values about 1 GOhm*cm for the wafers with diameter up to 3” and thickness up to 1000 um.

It has been established that the whole volume of the HR GaAs sensor is active.

It has been demonstrated that values of the $(\mu \cdot \tau)_n$ are about 10^{-4} cm^2/V.

It has been shown that the sensors provide a spatial resolution corresponding to the pixel pitch and allow obtaining of high quality X-ray images.

Future prospects are:

Design, produce, and testing pilot samples HR GaAs pixel sensors based on 4 inch GaAs wafers

Investigation of long-term stability of HR GaAs pixel sensors under X-ray irradiation

Thank you for your time !

Band gap modification

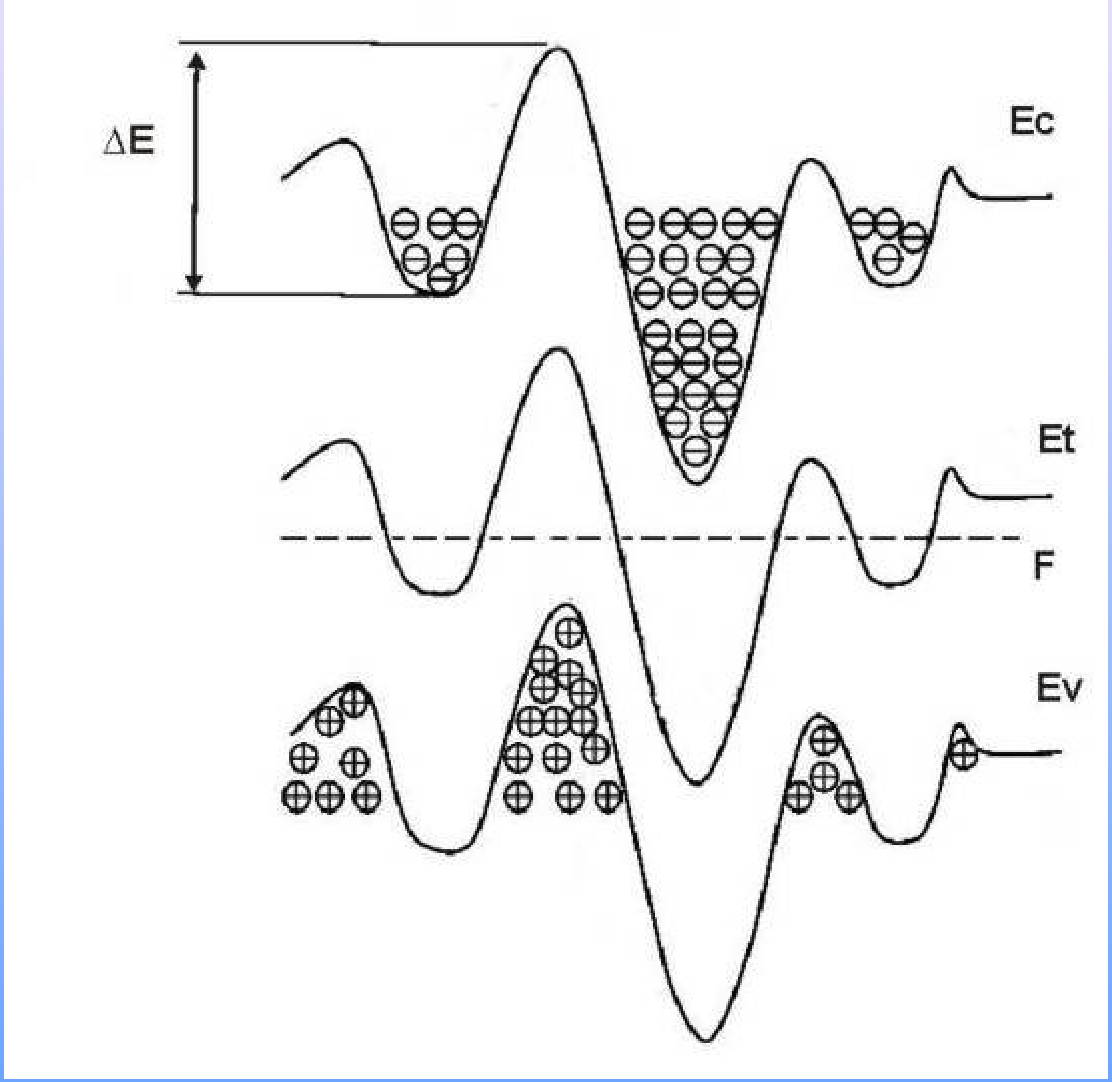

Analysis of
CCEβ,γ = f(Ubias)

$\mu_n\tau_n$: up to 10^{-4} cm^2/V

$\mu_p\tau_p$: 10^{-6} cm^2/V

τ_n: 50ns,
τ_p: 3ns.

$$\tau = \tau_0 \cdot \exp\left(\frac{\Delta E}{k \cdot T}\right)$$

$$\Delta E \approx 0.2 eV$$

Inhomogeneity of HR GaAs

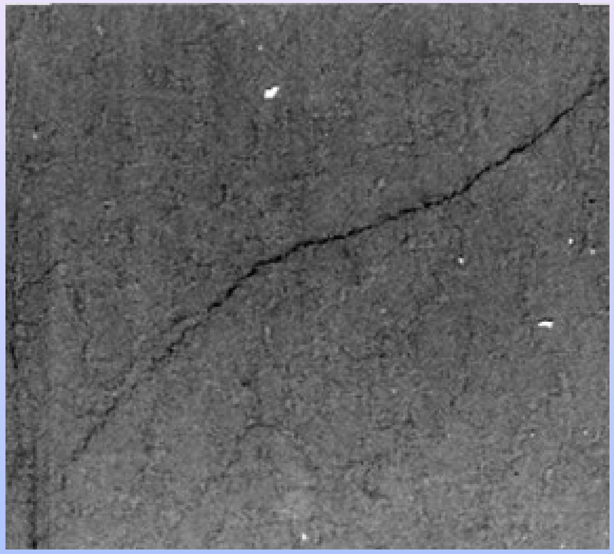

White beam topography of HR GaAs wafer [1]

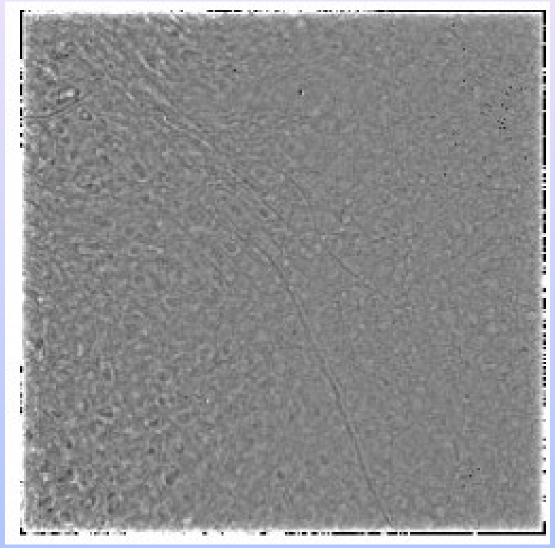

Flood image of a HR GaAs Timepix assembly [1]

[1]Procured by E. Hamann (IPS, Karlsruhe Institute of Technology, Eggenstein-Leopoldshafen, Germany)

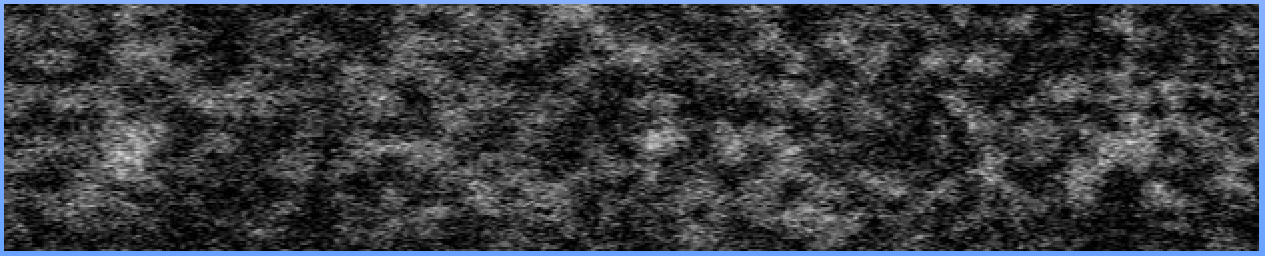

Inhomogeneity of HR GaAs based spatial light modulator luminescence

Distribution of the electric field strength in SI GaAs:EL2 sensor

400 V, t1

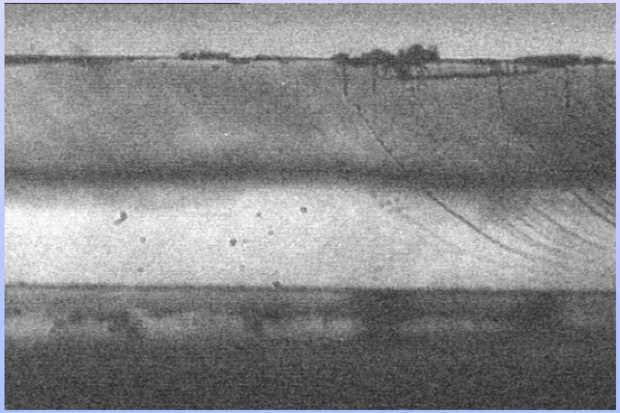

400 V, t2

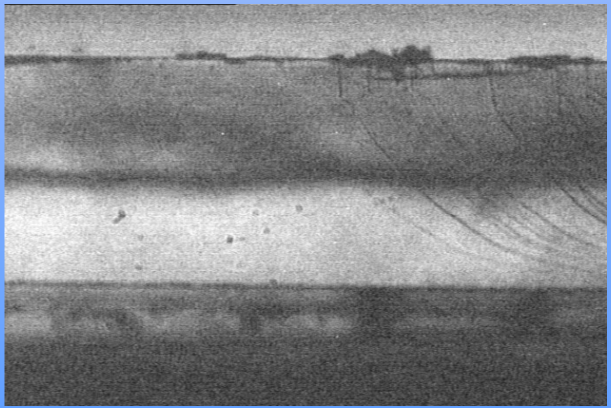

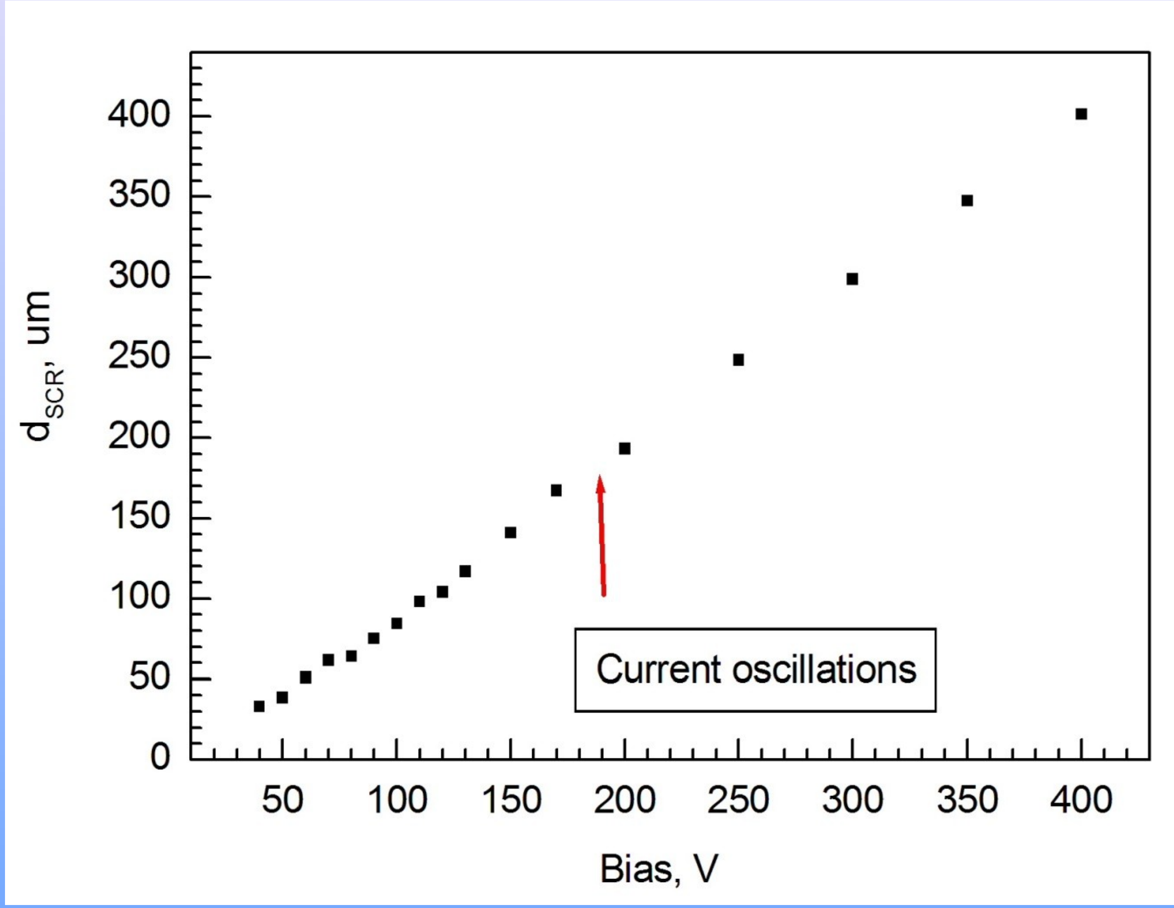

The temperature stability of the Ni contact HR GaAs pad sensors

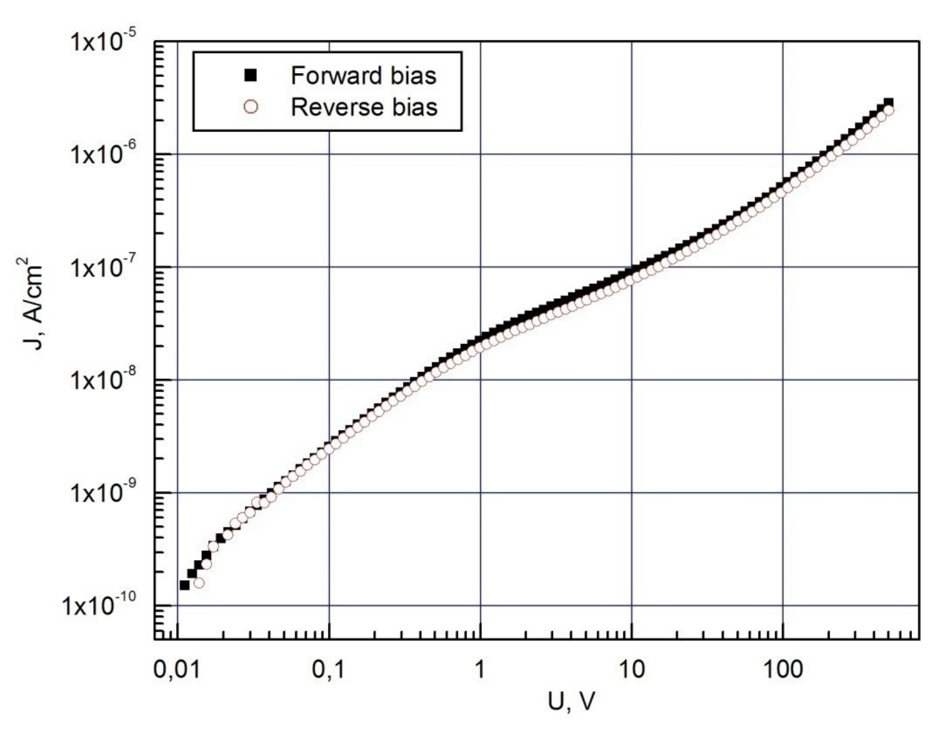

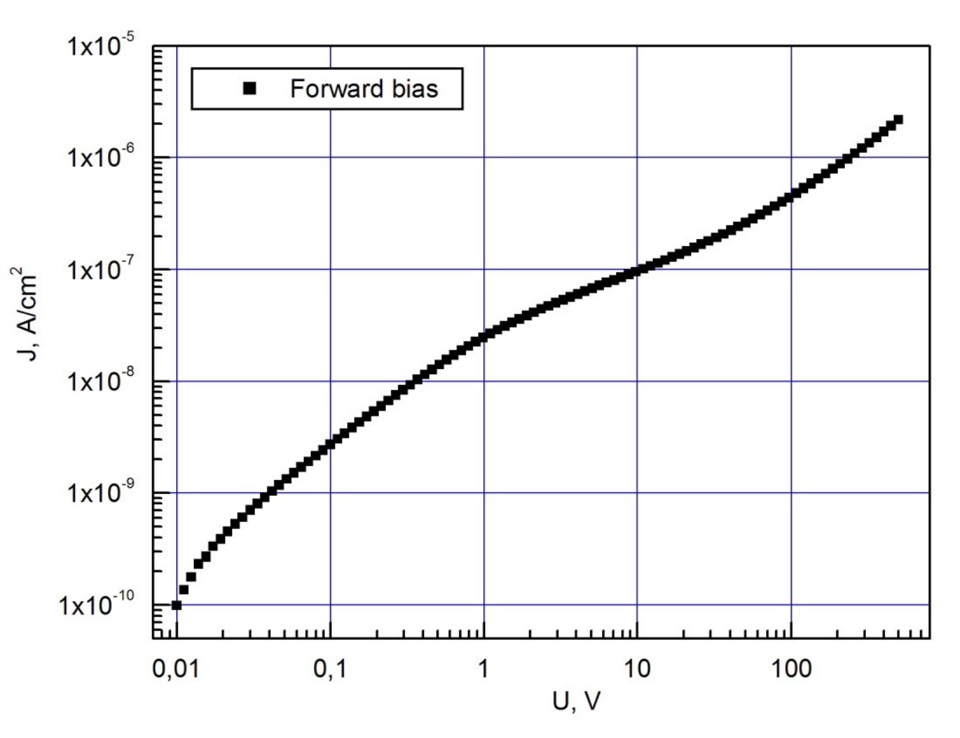

Sample annealed at 150 ºC in the atmosphere for 10 minutes

Sample annealed at 400 ºC in H_2 for 10 minutes

Resistivity of Ni - HR GaAs - Ni pad sensor

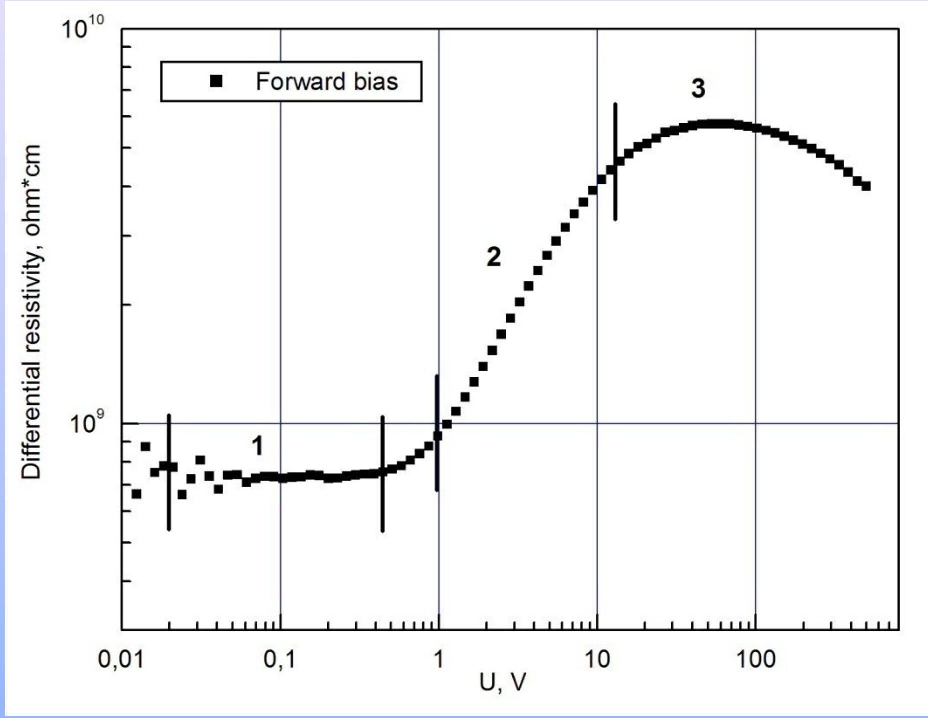

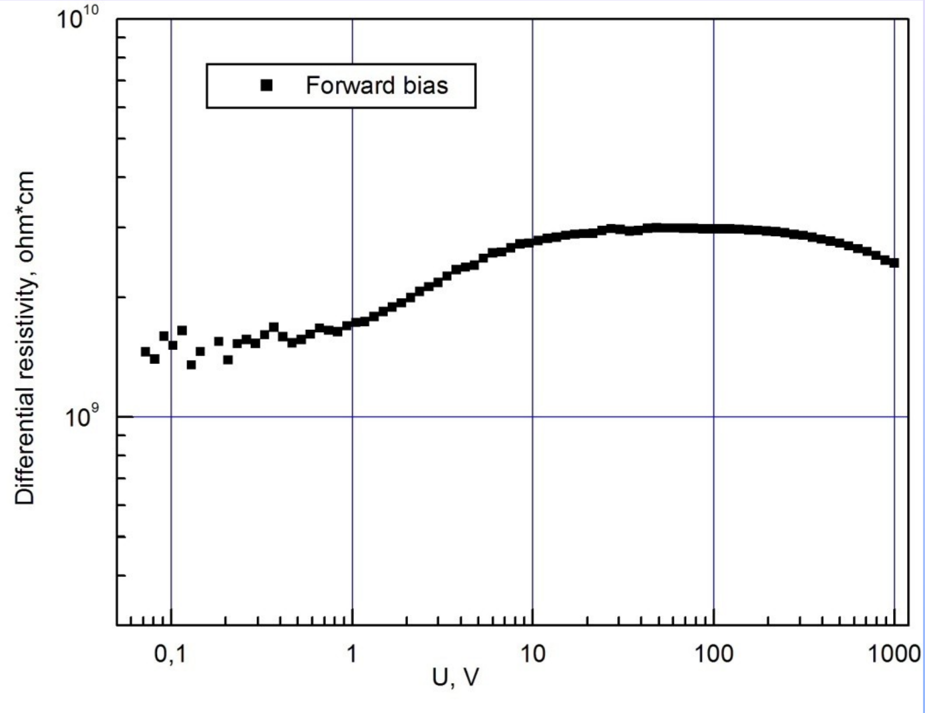

500 um thickness

980 um thickness

$$\rho_{diff} = \frac{1}{d} \cdot \left(\frac{dJ}{dU} \right)^{-1}$$

Simulation of the current-voltage characteristics

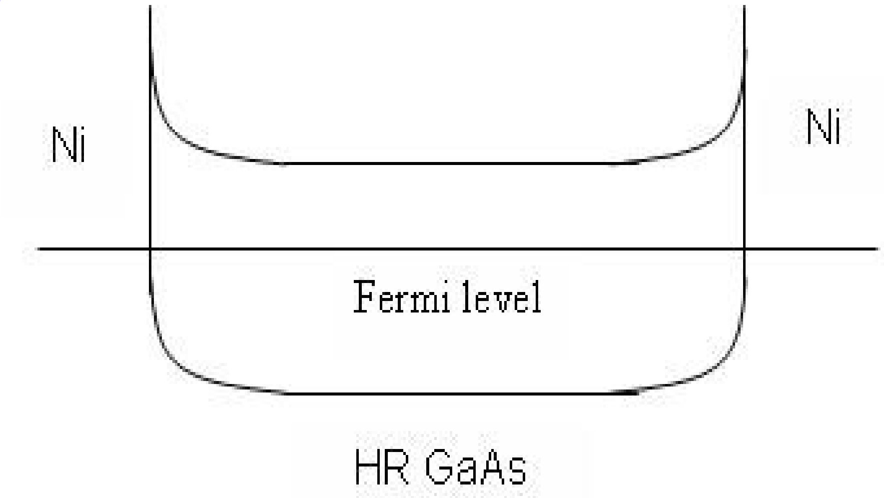

Band diagram of a HR GaAs pad sensor

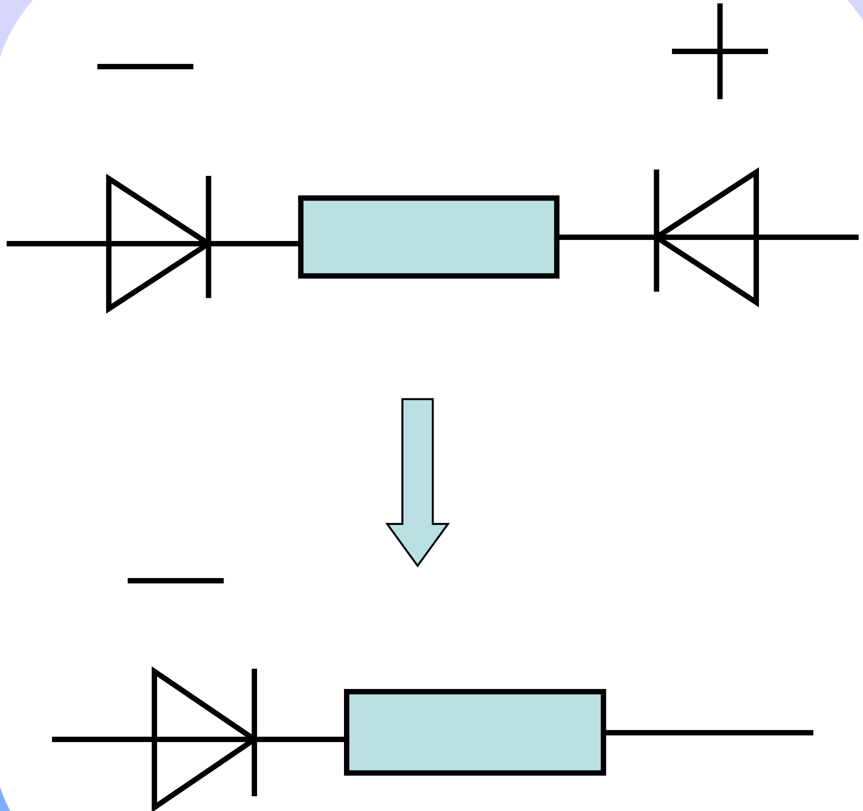

Equivalent circuit design

Calculated IV characteristics

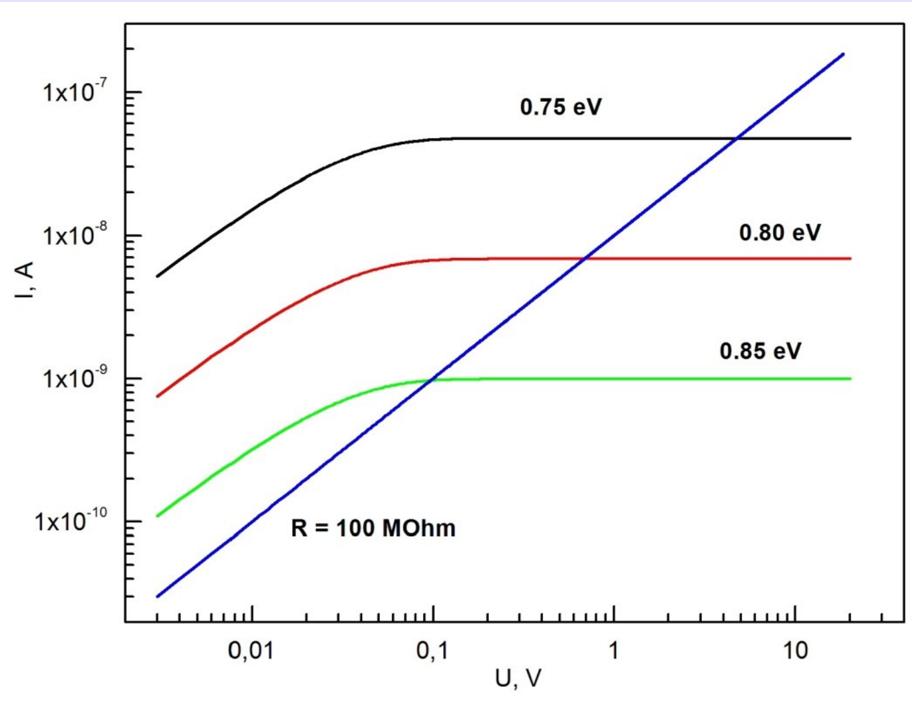

IV characteristics of reverse biased Schottky barrier with different φ_{b0} heights

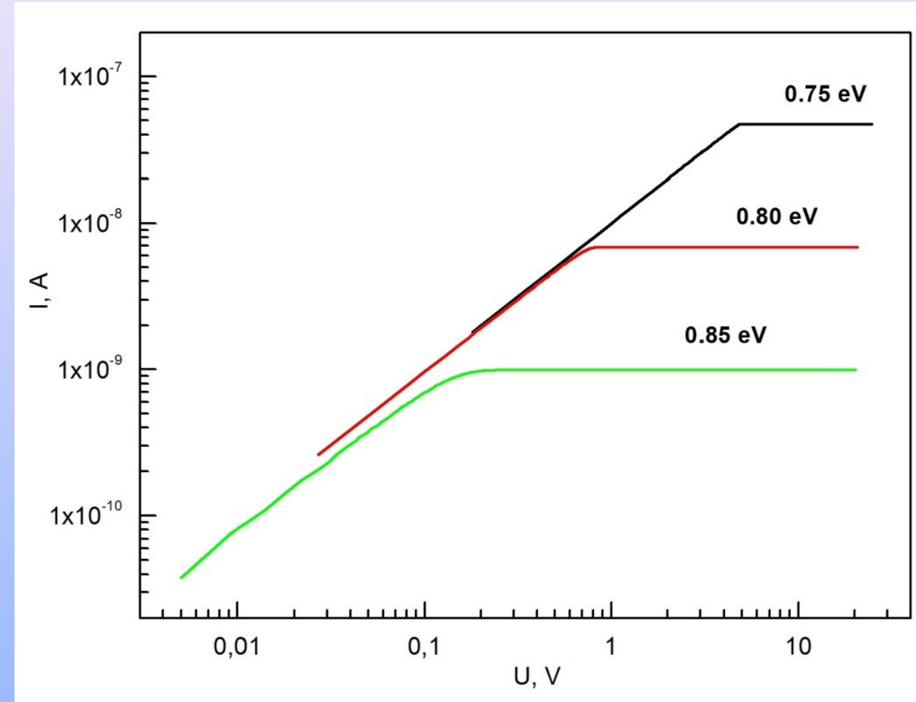

Calculated IV characteristics of the HR GaAs pad sensor

$$J = A^{*} \cdot T^{2} \cdot \exp\left(\frac{e \cdot \phi_{b0}}{k \cdot T}\right) \cdot \left[\exp\left(\frac{e \cdot U_{Schottky}}{k \cdot T}\right) - 1\right] = J_{st} \cdot \left[\exp\left(\frac{e \cdot U_{Schottky}}{k \cdot T}\right) - 1\right]$$

Potential barrier lowering.

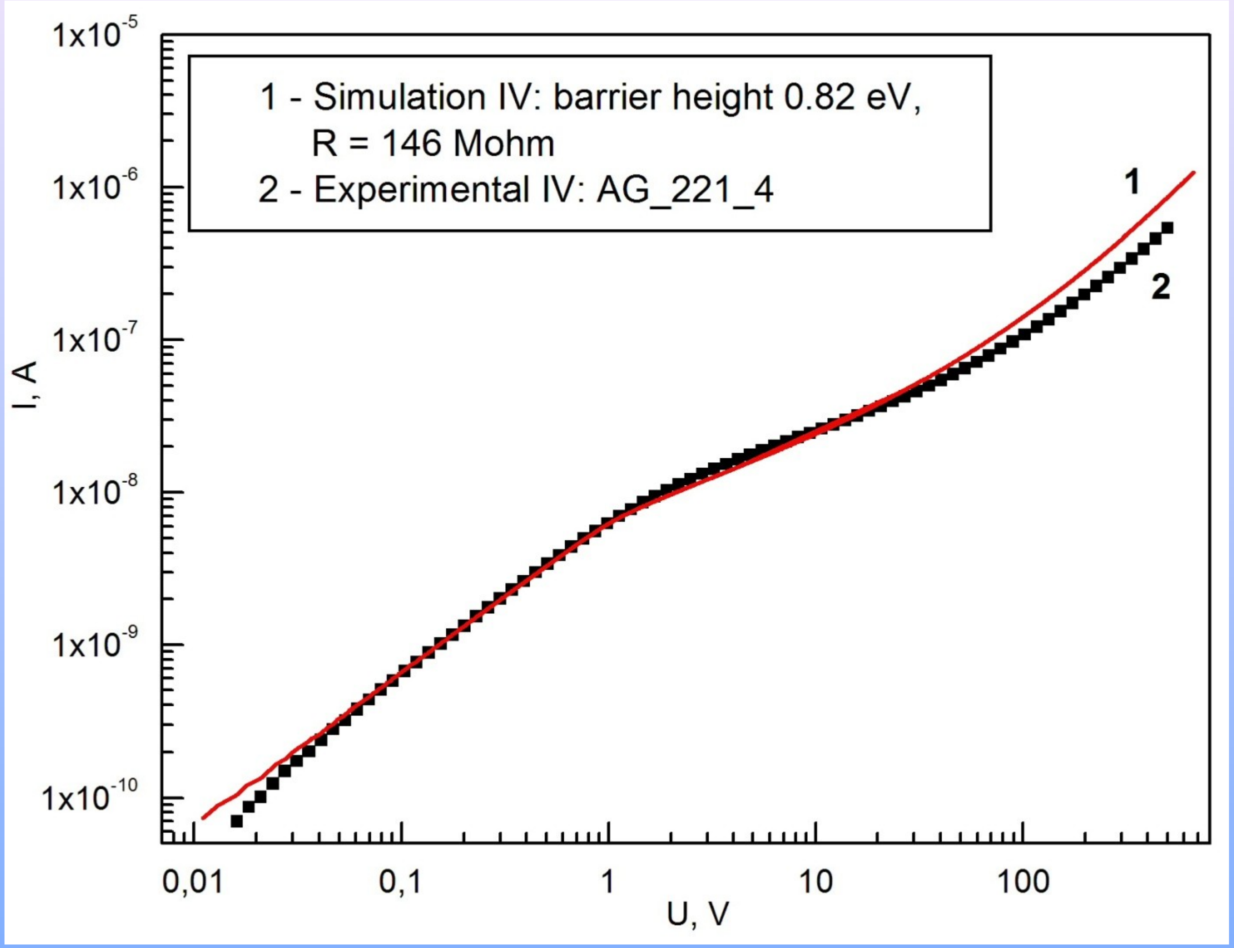

Calculated (1) IV characteristics of the HR GaAs pad sensor at $\varphi b0$ = 0.82 eV, R = 146 MOhm and the experimental (2) current-voltage characteristics the HR GaAs pad sensor.

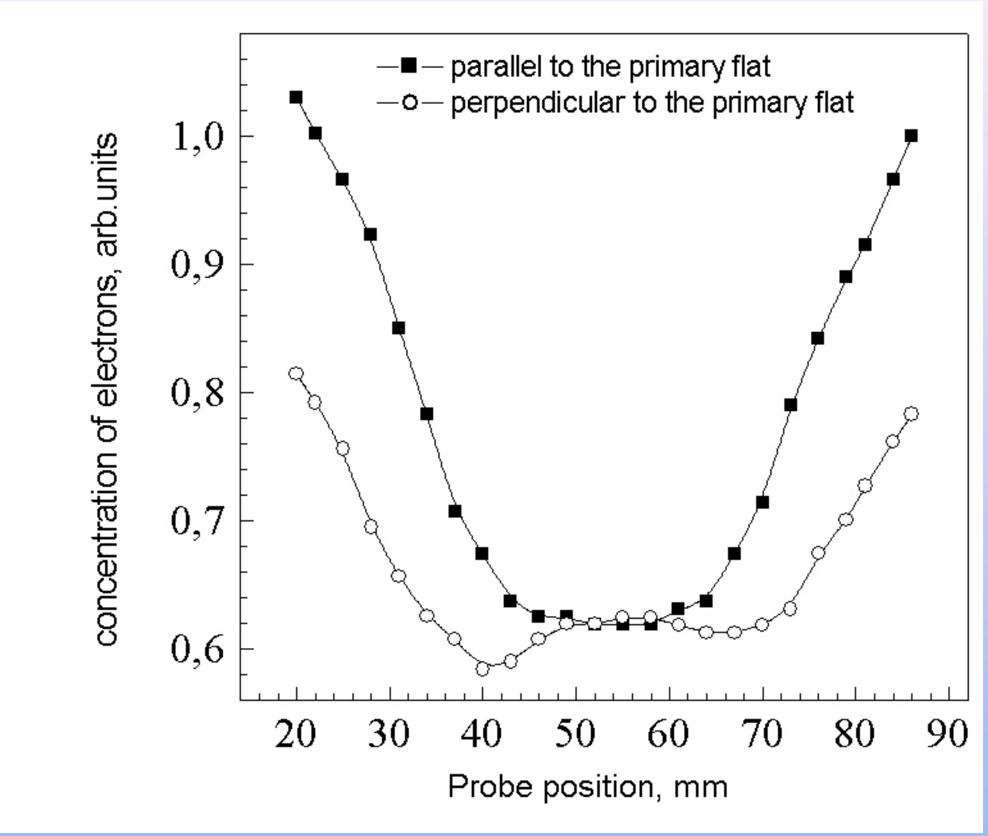

Charge carrier distribution on 40 and 76 mm diameter n- GaAs wafers. IR absorption.

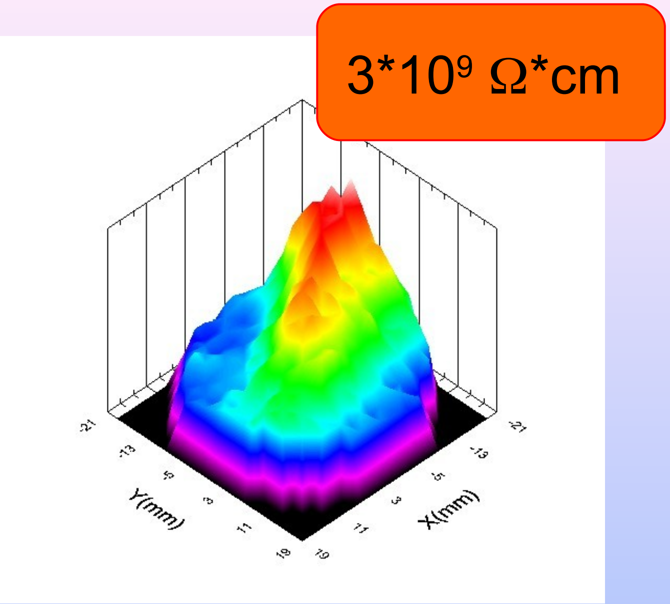

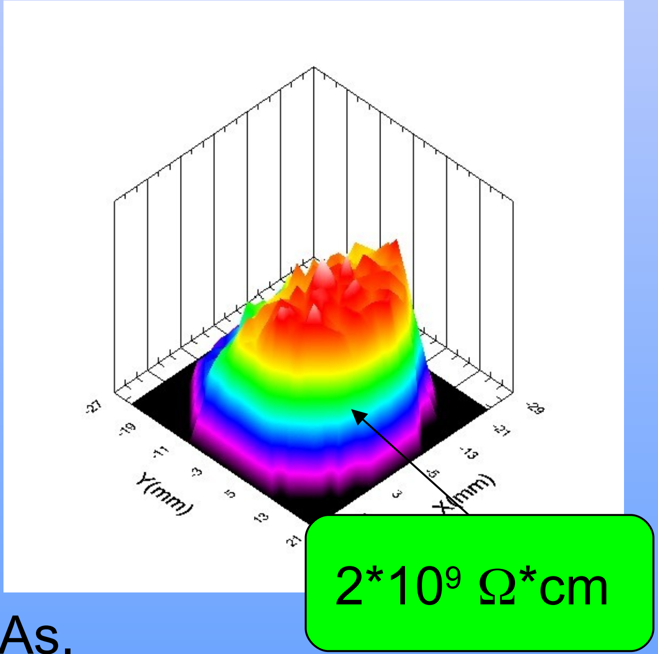

Resistivity distribution on 40mm HR GaAs.
EU-RHO-mutau-SCAN system

Evaluation of Detection Unit prototype for nondestructive testing

A pulsed X-ray source was used in the experiments. Average quantum energy of 3MeV, output pulse duration of 5μs, and pulse repetition frequency of 200 – 400Hz. The irradiation dose rate at the detector was 1.8R/min.

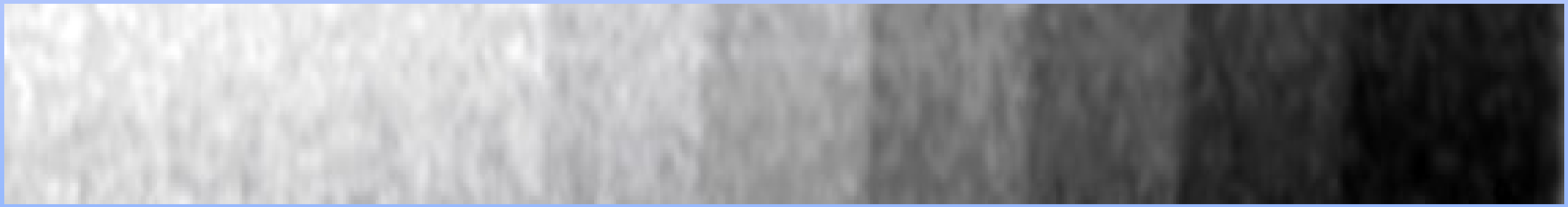

X-ray image of stack of 6 steel plates. The plates have 1.3, 6,12,18,24, and 30 mm in thickness. The stack was installed behind a steel 100mm thick absorber

Contrast of the system is ~ 3%

Evaluation of detection unit prototype for nondestructive testing

X-ray image of thin rod standard. The rod separation is 1mm and the rod thickness is 0.8mm

Spatial resolution of the system is about 1mm.

Evaluation of detection unit prototype for nondestructive testing

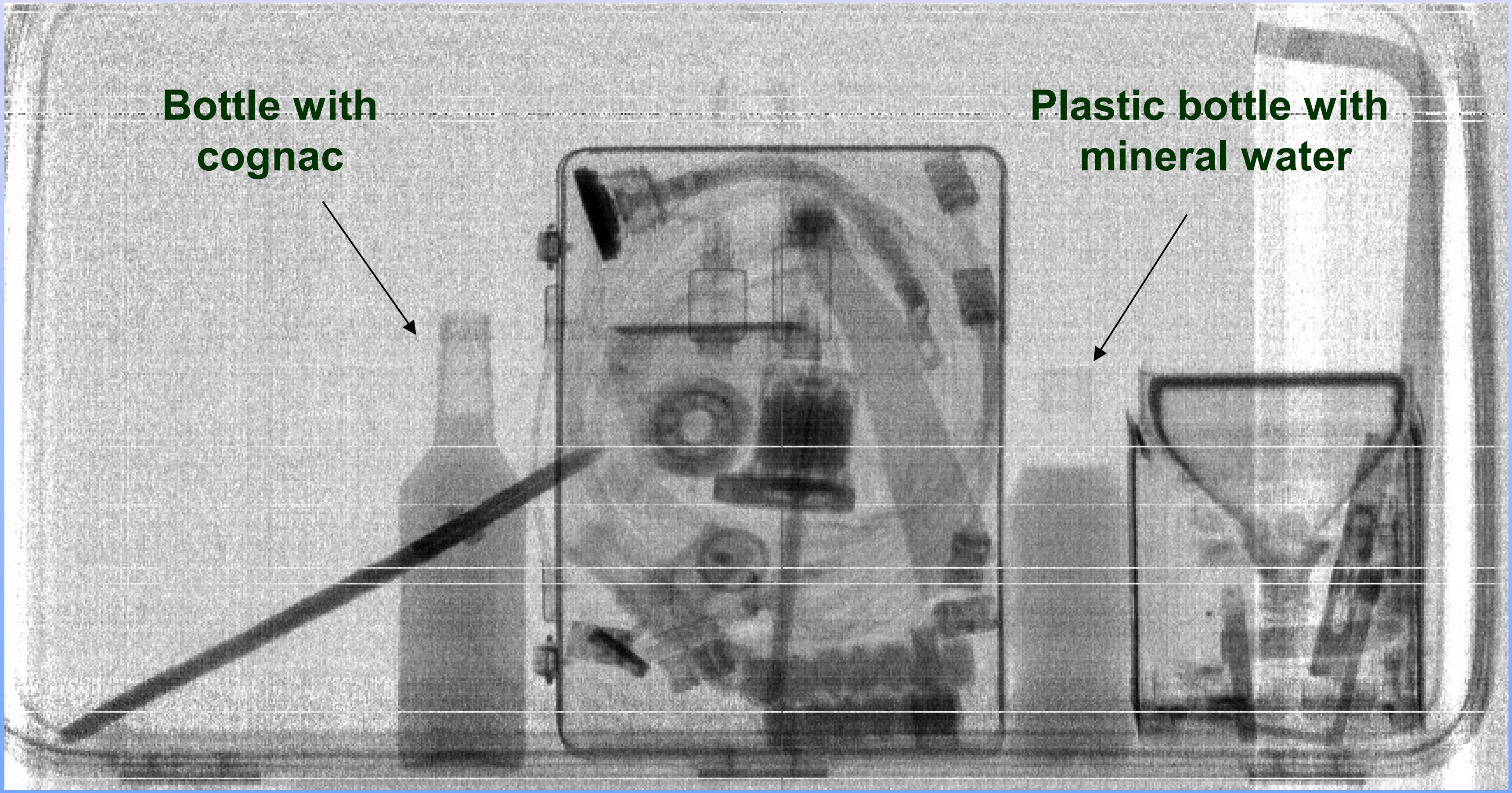

Different items inside metal box

Evaluation of detection unit prototype for nondestructive testing

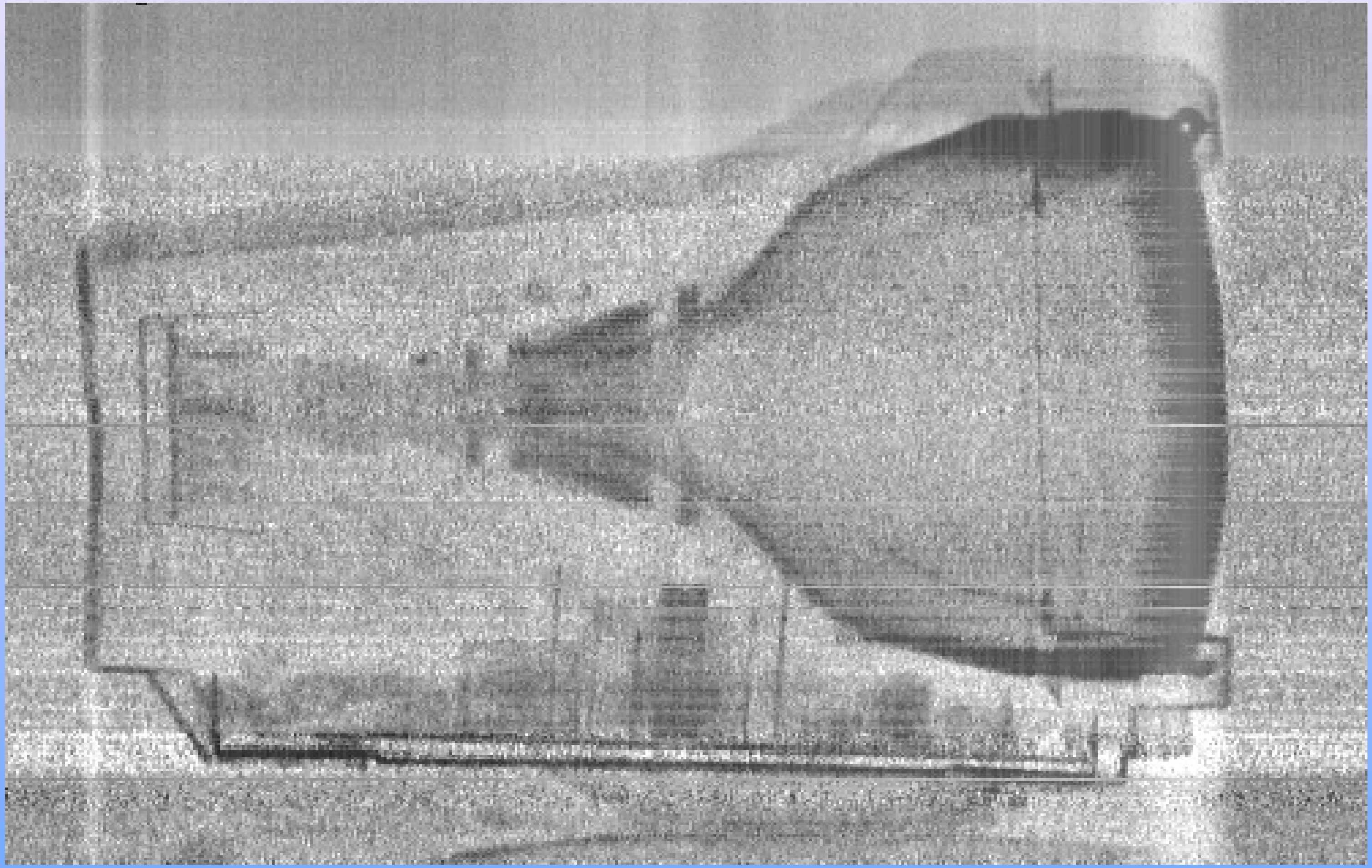

Image obtained through the steel sheet thickness being 50 mm

Radiation resistance: proton exposure (E_p = 1.7GeV)

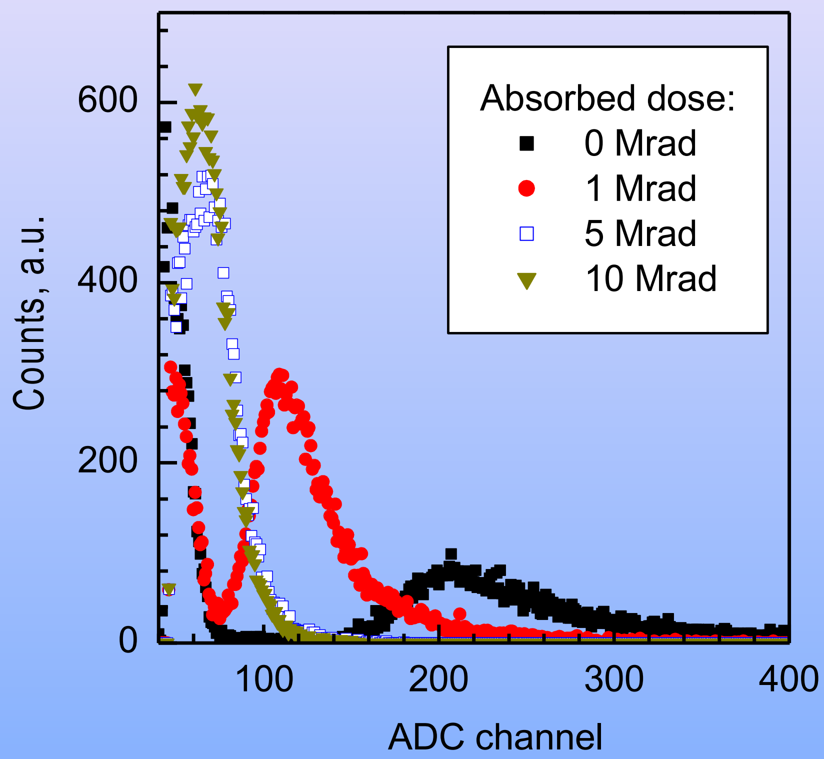

Figure 18. Dependence of the amplitude spectrum on the absorbed dose.

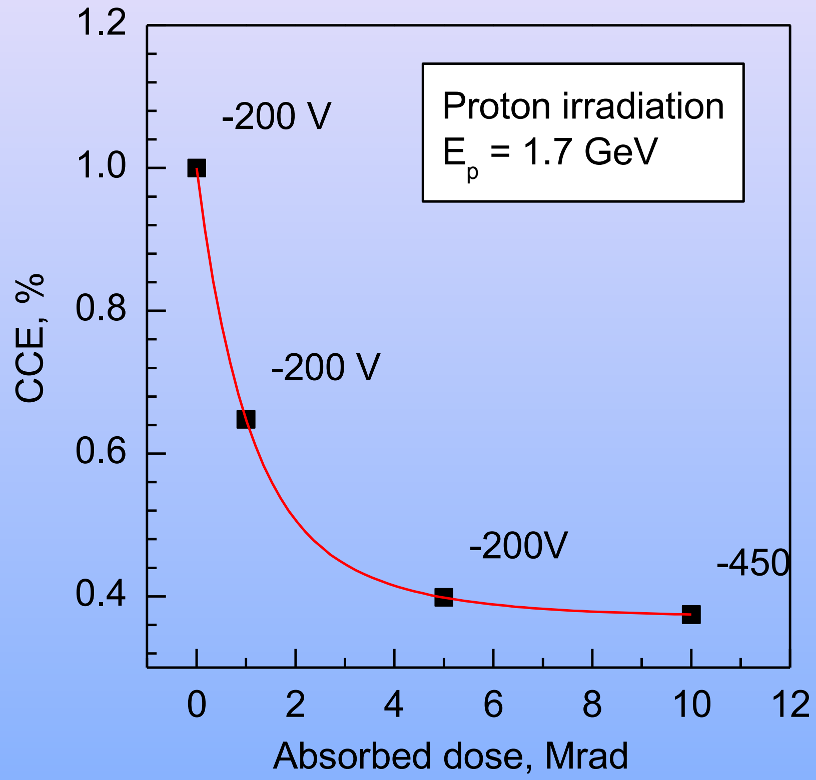

Figure 19. Dependence of the charge collection efficiency on the absorbed dose.